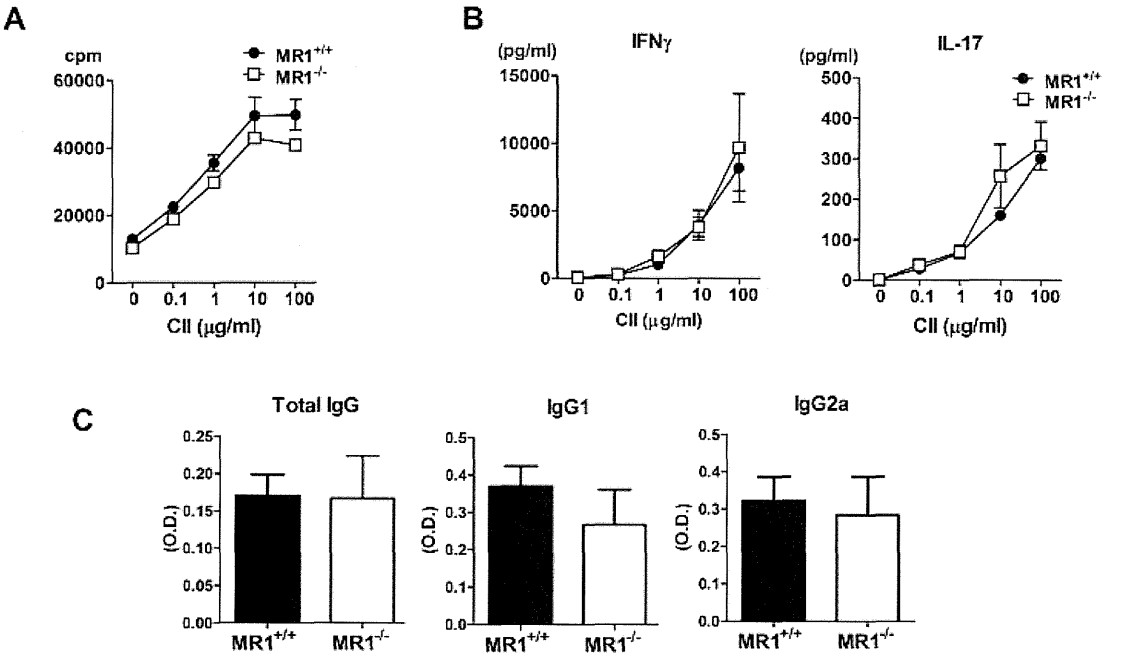

Figure 2. Type II collagen (CII) responses in $MR1^{-/-}$ DBA/1J mice. **A** and **B,** Inguinal lymph node cells from $MR1^{-/-}$ DBA/1J mice and $MR1^{+/+}$ DBA/1J mice with collagen-induced arthritis were incubated for 48 hours in the presence of CII. Proliferative responses were determined by the uptake of ^{3}H-thymidine (**A**), and the levels of interferon-γ (IFNγ) and interleukin-17 (IL-17) in culture supernatants were measured by enzyme-linked immunosorbent assay (**B**). **C,** CII-specific antibody levels in individual serum samples obtained at the end of the experiment were analyzed as described in Materials and Methods. Results from a single representative experiment of 2 similar experiments performed are shown. Values are the mean ± SEM of 5–8 mice per group. OD = optical density

the mean ± SEM clinical score for the group, and statistical differences were analyzed with a nonparametric Mann-Whitney U test. Data for cytokines and proliferation were analyzed with an unpaired *t*-test.

RESULTS

Amelioration of CIA in $MR1^{-/-}$ mice. To investigate whether MAIT cells play a role in the pathogenesis of arthritis, we first evaluated the involvement of MAIT cells in CIA using $MR1^{-/-}$ mice lacking MAIT cells. Because DBA/1J mice bearing the H-2q haplotype are the most susceptible strain for CIA, $MR1^{-/-}$ C57BL/6J mice were backcrossed to DBA/1J mice for 10 generations to obtain $MR1^{-/-}$ DBA/1J mice. Both $MR1^{-/-}$ DBA/1J mice and littermate $MR1^{+/+}$ DBA/1J mice were immunized with CII to induce CIA, and the clinical severity of arthritis was evaluated by visual scoring of each paw. As shown in Figure 1A, the clinical scores in $MR1^{-/-}$ DBA/1J mice were reduced in comparison to those in $MR1^{+/+}$ DBA/1J mice. Histologic examination of the joints of the 4 paws 44 days after CIA induction showed less cell infiltration, cartilage erosion, and bone destruction in $MR1^{-/-}$ DBA/1J mice than in the $MR1^{+/+}$ DBA/1J mice (Figure 1B). Quantification of the histologic severity of arthritis revealed that $MR1^{-/-}$ DBA/1J mice developed milder joint inflammation than $MR1^{+/+}$ DBA/1J mice (Figure 1C). These results suggest that MAIT cells contribute to the exacerbation of the disease course of CIA.

CII responses in $MR1^{-/-}$ DBA/1J mice. As the presence of MAIT cells augmented the severity of CIA, we next asked whether MAIT cells influence the CII-specific responses of T and B cells. Lymph node cells from CIA-induced animals were rechallenged with CII ex vivo. As shown in Figure 2A, the proliferative responses of lymph node cells upon stimulation with CII were similar in the two groups. Lymph node cells from both $MR1^{-/-}$ DBA/1J mice and $MR1^{+/+}$ DBA/1J mice produced comparable amounts of IL-17 and IFNγ in response to CII in a dose-dependent manner (Figure 2B). We also evaluated CII-specific immunoglobulin levels in serum obtained 35-42 days after arthritis induction. We observed a trend of reduced levels of CII-specific IgG1 in $MR1^{-/-}$ DBA/1J mice compared to the

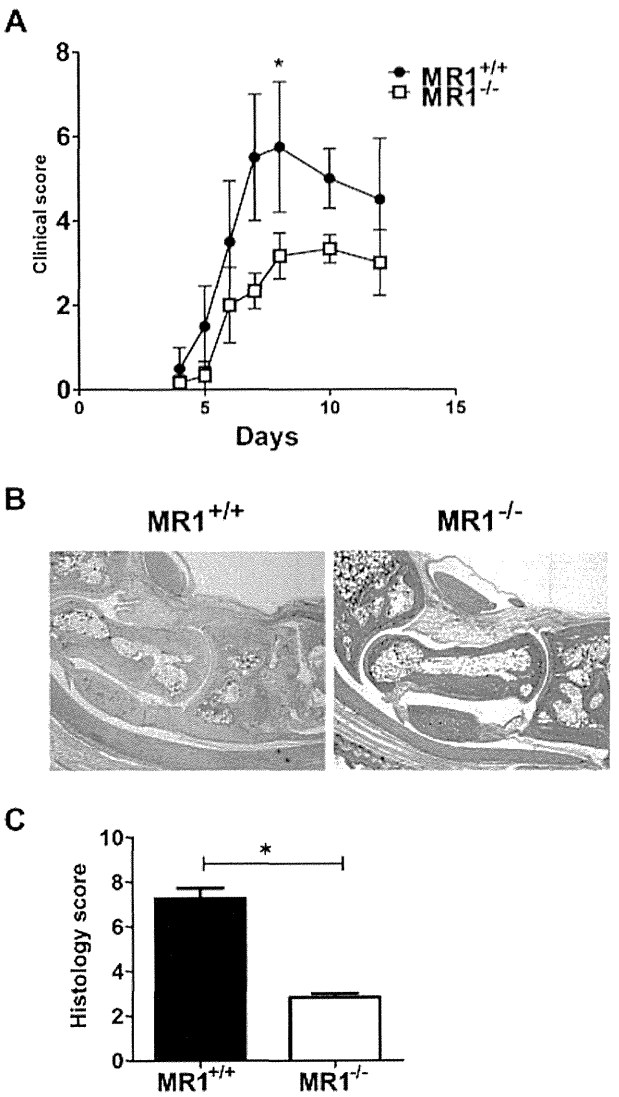

Figure 3. Amelioration of collagen antibody–induced arthritis (CAIA) in $MR1^{-/-}$ mice. **A,** Clinical scores for CAIA in $MR1^{-/-}$ C57BL/6J mice and $MR1^{+/+}$ C57BL/6J mice. Values are the mean ± SEM of 4–6 mice per group. * = $P < 0.05$ versus $MR1^{-/-}$ C57BL/6J mice. **B,** Representative histologic sections of the joints of $MR1^{+/+}$ C57BL/6J mice and $MR1^{-/-}$ C57BL/6J mice. Hematoxylin and eosin stained; original magnification × 40. **C,** Histology scores in $MR1^{-/-}$ C57BL/6J mice and in $MR1^{+/+}$ C57BL/6J mice, expressed as the sum of the scores in the 4 paws. Results from a single representative experiment of 2 similar experiments performed are shown. Values are the mean ± SEM. * = $P < 0.05$.

levels in $MR1^{+/+}$ DBA/1J mice, but the difference did not reach statistical significance (Figure 2C). These results indicate that the presence of MAIT cells has little effect on CII-specific responses.

Amelioration of CAIA in $MR1^{-/-}$ mice. The CIA model requires both adaptive and innate immune responses for disease development, and T cells and B cells responding to CII are the major players in the initiation of the disease. Although we observed significant differences in both the clinical and pathologic severity of arthritis when comparing $MR1^{-/-}$ DBA/1J mice to $MR1^{+/+}$ DBA/1J mice (Figure 1), the CII-specific responses of T and B cells appeared not to depend on the presence of MAIT cells (Figure 2). Thus, we hypothesized that MAIT cells may influence the effector phase of arthritis. To test this hypothesis, we induced CAIA in $MR1^{-/-}$ and $MR1^{+/+}$ C57BL/6J mice. By 7 days after injection of anti-CII mAb, $MR1^{+/+}$ C57BL/6J mice had developed severe arthritis, as assessed by clinical scores (Figure 3A). In contrast, the clinical scores in the $MR1^{-/-}$ C57BL/6J mice were lower compared to those in the $MR1^{+/+}$ C57BL/6J mice. Histologic assessment 10 days after arthritis induction revealed severe arthritis with leukocyte infiltration, synovial hyperplasia, pannus formation, cartilage erosion, and bone destruction in $MR1^{+/+}$ C57BL/6J mice, whereas these features were milder in $MR1^{-/-}$ C57BL/6J mice (Figures 3B and C).

Augmentation of arthritis in $MR1^{-/-}$ mice by adoptive transfer of MAIT cells. To demonstrate that MAIT cells actually enhance disease severity in the

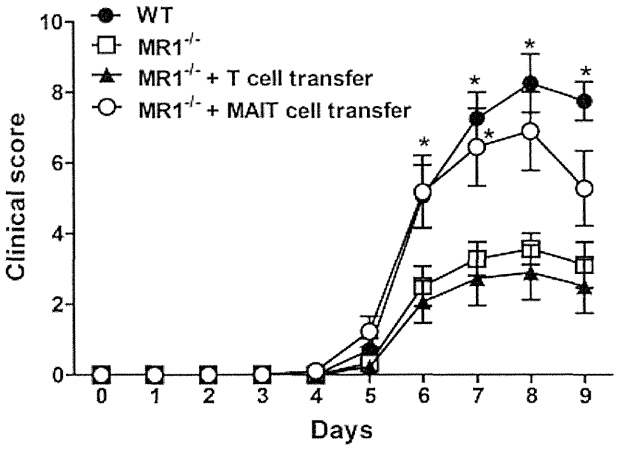

Figure 4. Augmentation of arthritis by adoptive transfer of mucosal-associated invariant T (MAIT) cells in $MR1^{-/-}$ mice. $MR1^{-/-}$ C57BL/6J mice received 5×10^5 NK1.1+TCRβ+ T cells (MAIT cells) or an equal number of NK1.1–TCRβ+ cells (T cells) from V_α19-transgenic $CD1d1^{-/-}$ mice. One day later, collagen antibody–induced arthritis was induced in wild-type (WT) C57BL/6J mice, $MR1^{-/-}$ C57BL/6J mice, and $MR1^{-/-}$ C57BL/6J mice reconstituted with T cells or MAIT cells. Results pooled from 2 similar experiments performed are shown. Values are the mean ± SEM of 8–10 mice per group. * = $P < 0.05$ versus $MR1^{-/-}$ C57BL/6J mice.

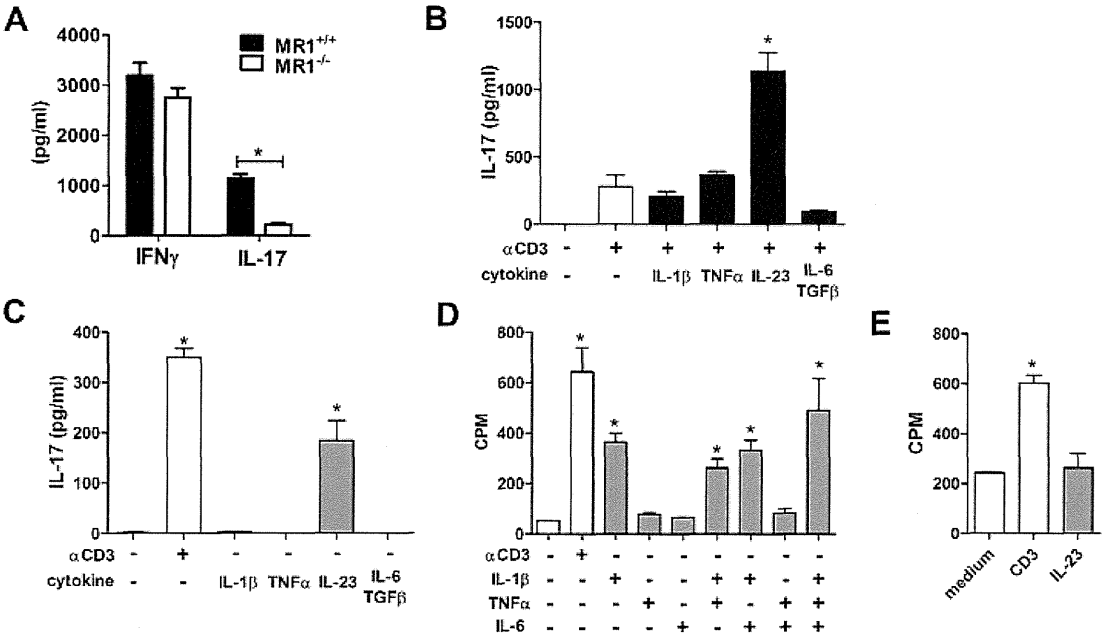

Figure 5. Cytokine-mediated mucosal-associated invariant T (MAIT) cell activation. **A,** Liver mononuclear cells from $MR1^{+/+}$ C57BL/6J mice and $MR1^{-/-}$ C57BL/6J mice were stimulated for 48 hours with immobilized anti-CD3 (αCD3) monoclonal antibody (mAb). The levels of interferon-γ (IFNγ) and interleukin-17 (IL-17) in culture supernatants were measured by enzyme-linked immunosorbent assay (ELISA). * = $P < 0.05$. **B,** MAIT cells were stimulated for 48 hours with immobilized anti-CD3 mAb, with or without IL-1β, tumor necrosis factor α (TNFα), IL-23, or IL-6 plus transforming growth factor β (TGFβ), and the levels of IL-17 were measured by ELISA. * = $P < 0.05$ versus anti-CD3 mAb stimulation alone. **C,** MAIT cells were stimulated with immobilized anti-CD3 mAb or the indicated cytokines, and IL-17 levels were measured. * = $P < 0.05$ versus unstimulated control. **D** and **E,** Proliferative responses after 48 hours of exposure to the indicated cytokines were determined as the uptake of ^{3}H-thymidine. Results from a single representative experiment of 2 similar experiments performed are shown. * = $P < 0.05$ versus unstimulated control. Values in **A–E** are the mean ± SEM.

CAIA model, we performed adoptive transfer experiments. Most NK1.1+ TCRβ T cells within liver lymphocytes from $CD1d1^{+/+}$ mice are iNKT cells, and we and other investigators previously demonstrated that the NK1.1+ TCRβ T cell population in V_α19i-transgenic $CD1d1^{-/-}$ mice is highly enriched in V_α19i TCR+ cells (15,17). Thus, to obtain MAIT cells, we isolated NK1.1+ TCRβ T cells from V_α19i-transgenic $CD1d1^{-/-}$ mice. We adoptively transferred these MAIT cells into $MR1^{-/-}$ C57BL/6J mice, and 1 day later, we injected these mice with anti-CII mAb to induce CAIA. $MR1^{-/-}$ C57BL/6J mice reconstituted with MAIT cells developed severe arthritis at a level similar to that of wild-type (WT) C57BL/6J mice (Figure 4). However, the transfer of an equal number of T cells into $MR1^{-/-}$ C57BL/6J mice had little effect on the clinical arthritis scores. Taken together, these results suggest that the presence of MAIT cells augmented arthritis mainly by enhancing the inflammation in arthritis.

Cytokine-mediated MAIT cell activation. To understand the mechanism by which MAIT cells exacerbate the disease course of arthritis, we first compared the cytokine-producing capacity of T cells from $MR1^{-/-}$ and WT C57BL/6J mice. Upon anti-CD3 mAb stimulation, LMNCs from $MR1^{-/-}$ and WT C57BL/6J mice produced comparable amounts of IFNγ. However, the level of IL-17 was lower in $MR1^{-/-}$ C57BL/6J mice than in WT C57BL/6J mice (Figure 5A).

It was recently demonstrated that human MAIT cells express the Th17-associated transcription factor retinoic acid receptor–related orphan nuclear receptor (ROR) and produce high levels of IL-17 (33). We therefore sought to determine whether mouse MAIT cells produce IL-17, which is known to play a pathogenic role in arthritis. MAIT cells were sorted from LMNCs obtained from V_α19i-transgenic $CD1d1^{-/-}$ mice and were stimulated ex vivo with anti-CD3 mAb. As previously shown (34), MAIT cells produced large amounts of IL-17. In addition, IL-17 production by anti-CD3 mAb–stimulated MAIT cells was augmented in the presence of IL-23 (Figure 5B).

Innate-like lymphocytes such as iNKT cells and

γ/δ T cells are known to be activated by cytokines directly, without TCR stimulation. A combination of IL-12 and IL-18 activates iNKT cells to produce IFNγ, and IL-1 together with IL-23 induces IL-17 production by γ/δ T cells (31,35,36). We therefore next asked whether MAIT cells are activated directly by cytokines. MAIT cells were incubated with various cytokines without TCR stimulation, and cytokine concentrations in the culture supernatants were evaluated. Surprisingly, MAIT cells produced high levels of IL-17 after exposure to IL-23 in the absence of TCR stimulation (Figure 5C).

Inflammatory cytokines such as IL-1β, TNFα, and IL-6 play critical roles in arthritis models and in human RA. Therefore, we next tested whether MAIT cells could be activated by these cytokines. As shown in Figure 5D, IL-1β induced robust proliferation of MAIT cells, although cytokine production was not observed after exposure to these cytokines, including IL-1β (data not shown). In addition, IL-23 did not induce proliferation of MAIT cells (Figure 5E). Thus, in the absence of TCR stimuli, IL-1β induced the proliferation of MAIT cells and IL-23 promoted the production of IL-17 by MAIT cells.

DISCUSSION

Previous studies by our group as well as others revealed that iNKT cells play pathogenic roles in CIA and CAIA by inducing a Th1 or Th17 shift of autoimmune T cells and by augmenting the inflammation in arthritis (25–27). In the present study, we demonstrated that MAIT cells contribute to the severity of CIA and CAIA mostly by augmenting joint inflammation during the effector phase of arthritis. $MR1^{-/-}$ mice were originally generated on the 129P2 background. Although $MR1^{-/-}$ mice were backcrossed onto C57BL/6 or DBA/1J, we are not able to exclude the possibility that some residual sequence from the 129P2 mice affects the arthritis susceptibility of $MR1^{-/-}$ C57BL/6 and $MR1^{-/-}$ DBA/1J mice. However, since the reconstitution of MAIT cells induced severe CAIA in $MR1^{-/-}$ C57BL/6 mice, the phenotype observed in $MR1^{-/-}$ mice seems to be dependent on the lack of MAIT cells.

It has been revealed that there are CD1d-restricted T cells that are different from iNKT cells and do not express an invariant TCRα chain ($V_\alpha14$–$J_\alpha18$ in mice and $V_\alpha24$–$J_\alpha18$ in humans). Such CD1d-restricted T cells are called type II NKT cells and possess different functions from iNKT cells. Recently, CD1d-restricted NKT cells, which recognize murine type II collagen peptide 707–721, were reported to suppress CIA (37). It is not known whether there are distinct subsets with different functions among MAIT cells or whether there are other T cells that are restricted by the MR1 molecule. As adoptively transferred $V_\alpha19i$ T cells augmented CAIA in $MR1^{-/-}$ mice, MAIT cells include the population that enhances the inflammation in arthritis.

It was recently shown that IL-17–producing γ/δ T cells were observed in the joints of mice with CIA and that blocking a certain subset of IL-17–producing γ/δ T cells suppressed CIA (29). However, γ/δ T cells have been shown to be dispensable for the development of CIA (38). In addition, anti-CII–specific antibody levels were comparable between γ/δ T cell–deficient and wild-type mice. These findings suggest that MAIT cells and γ/δ T cells share similar roles in arthritis and that both are involved mainly in the effector phase of arthritis. It is known that γ/δ T cells as well as iNKT cells are increased during CIA. Because MAIT cells share similar features with γ/δ T cells and iNKT cells, MAIT cells may also be increased during CIA.

We observed a significant decrease in IL-17 production by LMNCs upon stimulation with anti-CD3 mAb in $MR1^{-/-}$ mice compared to WT control mice. As sorted MAIT cells produced high amounts of IL-17 after anti-CD3 mAb stimulation, the major source of IL-17 responsible for the difference between $MR1^{-/-}$ and WT mice seems to be MAIT cells. Th17 cells and iNKT cells have been shown to produce IL-21, which enhanced IL-17 production or induced proliferation of IL-17–producing cells (39). It is not known whether MAIT cells produce IL-21, but MAIT cells might augment IL-17 production by other LMNCs, including γ/δ T cells, through such mechanisms. Further studies to determine whether MAIT cells regulate γ/δ T cells under both physiologic and pathologic conditions, including in the presence of arthritis, will be of interest.

The frequency of murine γ/δ T cells is 1–5% in blood lymphocytes and 25–60% in gut lymphocytes. Human γ/δ T cells also comprise up to 2–3% of peripheral T cells (9,10). Although the precise frequency of murine MAIT cells is not known, it has been speculated that MAIT cells may comprise up to 10% of double-negative T cells in the gut lamina propria and <2% of double-negative T cells in the mesenteric lymph nodes, indicating that the frequency of murine MAIT cells is much lower than that of mouse γ/δ T cells (15). It has been suggested that γ/δ T cells are the predominant source of IL-17 in the joints of CIA mice, but IL-17–producing γ/δ T cells could not be detected in RA synovial tissue (31). Recently, Martin et al (23) revealed that human MAIT cells can be identified as $V_\alpha7.2+$ $CD161^{high}$ T cells, which are abundant in blood. In addition, human MAIT cells produce IL-17 and express

tissue-homing chemokine receptors (23). An IL-17–producing CD161^{high} T cell population has been described in human arthritic joints (40). Thus, it is possible that MAIT cells rather than γ/δ T cells play a major role in the pathogenesis of human RA.

CD4+ Th17 cells require IL-6/STAT-3 activation for the expression of RORγt, which is a crucial transcription factor for IL-17 production (41). However, some innate-like lymphocyte subsets, such as iNKT cells, γ/δ T cells, and lymphoid tissue–inducer (LTi)–like cells, are known to constitutively express RORγt, IL-1 receptor type I, and IL-23R (42). In addition, these IL-17–producing innate-like lymphocytes, including LTi cells, γ/δ T cells, and iNKT cells, secrete IL-17 when stimulated by IL-23 with or without IL-1β. In this study, we demonstrated cytokine-mediated activation of MAIT cells. MAIT cells produced IL-17 in response to IL-23. Moreover, IL-1β induced proliferation of MAIT cells. Thus, it is possible that MAIT cells may contribute to the disease progression of arthritis through another mechanism in addition to IL-17 production. In adoptive transfer experiments, MAIT cells augmented the disease severity of CAIA in MR1-deficient mice. Thus, this result also indicates that MAIT cell–mediated exacerbation of arthritis may be induced by cytokines, without a requirement for TCR stimulation.

In EAE, disease suppression by MAIT cells was accompanied by a reduction in the production of cytokines, including IFNγ and IL-17, by T cells and increased IL-10 production by B cells. Encephalitogenic T cells play a major role in EAE (43,44). EAE can be induced in naive mice by transferring myelin-reactive T cells. T cell–targeted therapies, including anti–very late activation antigen 4 treatment, have been shown to suppress EAE. Although CIA was reduced in MR1$^{-/-}$ DBA/1J mice, we observed a significant decrease in CII-specific IgG1 antibody levels in these mice as compared with their WT controls in some experiments (data not shown), suggesting the inhibition of Th1 responses by MAIT cells. Therefore, it is still possible that MAIT cells suppress Th1 response during the early induction phase of CIA. MAIT cells may be functionally plastic, and thus exert different functions depending on the pathologic condition. Arthritis involves massive cytokine production due to various types of immune cell activation. Since MAIT cells can be activated by inflammatory cytokines, MAIT cells may contribute to augment the immune response once overt inflammation occurs.

In summary, we have shown that MAIT cells contribute to the progression of arthritis by enhancing the inflammation in CIA and CAIA models. In addition, we demonstrated that MAIT cells could be activated by cytokine stimulation even without TCR stimulation. We and others previously reported that, although iNKT cells play pathogenic roles in arthritis models, modulation of iNKT cell function by ligands successfully suppressed arthritis (45–47). The proportion of human MAIT cells appears to be much higher than that of mouse MAIT cells. Therefore, MAIT cells may play an important pathogenic role in human arthritis and MAIT cell–targeted therapy may hold promise as a new therapeutic intervention for arthritis, including RA.

ACKNOWLEDGMENTS

The authors thank S. Gilfillan (Washington University School of Medicine, St. Louis, MO) for MR1$^{-/-}$ mice and M. Shimamura (University of Tsukuba, Ibaraki, Japan) for $V_{\alpha}19$-transgenic mice.

AUTHOR CONTRIBUTIONS

All authors were involved in drafting the article or revising it critically for important intellectual content, and all authors approved the final version to be published. Dr. Miyake had full access to all of the data in the study and takes responsibility for the integrity of the data and the accuracy of the data analysis.

Study conception and design. Chiba, Tajima, Miyazaki, Miyake.
Acquisition of data. Chiba, Tajima, Tomi, Miyazaki.
Analysis and interpretation of data. Chiba, Tajima, Tomi, Miyazaki, Yamamura, Miyake.

REFERENCES

1. Chervonsky AV. Influence of microbial environment on autoimmunity [review]. Nat Immunol 2010;11:28–35.
2. Vaahtovuo J, Munukka E, Korkeamaki M, Luukkainen R, Toivanen P. Fecal microbiota in early rheumatoid arthritis. J Rheumatol 2008;35:1500–5.
3. Stone M, Fortin PR, Pacheco-Tena C, Inman RD. Should tetracycline treatment be used more extensively for rheumatoid arthritis? Metaanalysis demonstrates clinical benefit with reduction in disease activity. J Rheumatol 2003;30:2112–22.
4. Nieuwenhuis EE, Visser MR, Kavelaars A, Cobelens PM, Fleer A, Harmsen W, et al. Oral antibiotics as a novel therapy for arthritis: evidence for a beneficial effect of intestinal Escherichia coli. Arthritis Rheum 2000;43:2583–9.
5. Wu HJ, Ivanov II, Darce J, Hattori K, Shima T, Umesaki Y, et al. Gut-residing segmented filamentous bacteria drive autoimmune arthritis via T helper 17 cells. Immunity 2010;32:815–27.
6. Vivier E, Tomasello E, Baratin M, Walzer T, Ugolini S. Functions of natural killer cells [review]. Nat Immunol 2008;9:503–10.
7. Kronenberg M, Kinjo Y. Innate-like recognition of microbes by invariant natural killer T cells [review]. Curr Opin Immunol 2009;21:391–6.
8. Brigl M, Brenner MB. How invariant natural killer T cells respond to infection by recognizing microbial or endogenous lipid antigens [review]. Semin Immunol 2010;22:79–86.
9. Carding SR, Egan PJ. γδ T cells: functional plasticity and heterogeneity [review]. Nat Rev Immunol 2002;2:336–45.
10. Bonneville M, O'Brien RL, Born WK. γδ T cell effector functions: a blend of innate programming and acquired plasticity [review]. Nat Rev Immunol 2010;10:467–78.
11. Allman D, Pillai S. Peripheral B cell subsets [review]. Curr Opin Immunol 2008;20:149–57.

12. Lopes-Carvalho T, Foote J, Kearney JF. Marginal zone B cells in lymphocyte activation and regulation [review]. Curr Opin Immunol 2005;17:244–50.
13. Le Bourhis L, Guerri L, Dusseaux M, Martin E, Soudais C, Lantz O. Mucosal-associated invariant T cells: unconventional development and function [review]. Trends Immunol 2011;32:212–8.
14. Treiner E, Duban L, Bahram S, Radosavljevic M, Wanner V, Tilloy F, et al. Selection of evolutionarily conserved mucosal-associated invariant T cells by MR1. Nature 2003;422:164–9.
15. Kawachi I, Maldonado J, Strader C, Gilfillan S. MR1-restricted Vα19i mucosal-associated invariant T cells are innate T cells in the gut lamina propria that provide a rapid and diverse cytokine response. J Immunol 2006;176:1618–27.
16. Illes Z, Shimamura M, Newcombe J, Oka N, Yamamura T. Accumulation of Vα7.2-Jα33 invariant T cells in human autoimmune inflammatory lesions in the nervous system. Int Immunol 2004;16:223–30.
17. Croxford JL, Miyake S, Huang YY, Shimamura M, Yamamura T. Invariant Vα19i T cells regulate autoimmune inflammation. Nat Immunol 2006;7:987–94.
18. Peterfalvi A, Gomori E, Magyarlaki T, Pal J, Banati M, Javorhazy A, et al. Invariant Vα7.2-Jα33 TCR is expressed in human kidney and brain tumors indicating infiltration by mucosal-associated invariant T (MAIT) cells. Int Immunol 2008;20:1517–25.
19. Gold MC, Cerri S, Smyk-Pearson S, Cansler ME, Vogt TM, Delepine J, et al. Human mucosal associated invariant T cells detect bacterially infected cells. PLoS Biol 2010;8:e1000407.
20. Le Bourhis L, Martin E, Peguillet I, Guihot A, Froux N, Core M, et al. Antimicrobial activity of mucosal-associated invariant T cells. Nat Immunol 2010;11:701–8.
21. Tilloy F, Treiner E, Park SH, Garcia C, Lemonnier F, de la Salle H, et al. An invariant T cell receptor α chain defines a novel TAP-independent major histocompatibility complex class IB-restricted α/β T cell subpopulation in mammals. J Exp Med 1999; 189:1907–21.
22. Lantz O, Bendelac A. An invariant T cell receptor α chain is used by a unique subset of major histocompatibility complex class I-specific CD4+ and CD4−CD8− T cells in mice and humans. J Exp Med 1994;180:1097–106.
23. Martin E, Treiner E, Duban L, Guerri L, Laude H, Toly C, et al. Stepwise development of MAIT cells in mouse and human. PLoS Biol 2009;7:e54.
24. Lo CK, Lam QL, Sun L, Wang S, Ko KH, Xu H, et al. Natural killer cell degeneration exacerbates experimental arthritis in mice via enhanced interleukin-17 production. Arthritis Rheum 2008;58: 2700–11.
25. Chiba A, Kaieda S, Oki S, Yamamura T, Miyake S. The involvement of $V_{\alpha}14$ natural killer T cells in the pathogenesis of arthritis in murine models. Arthritis Rheum 2005;52:1941–8.
26. Kim HY, Kim HJ, Min HS, Kim S, Park WS, Park SH, et al. NKT cells promote antibody-induced joint inflammation by suppressing transforming growth factor β1 production. J Exp Med 2005;201: 41–7.
27. Ohnishi Y, Tsutsumi A, Goto D, Itoh S, Matsumoto I, Taniguchi M, et al. TCR Vα14 natural killer T cells function as effector T cells in mice with collagen-induced arthritis. Clin Exp Immunol 2005;141:47–53.
28. Teige A, Bockermann R, Hasan M, Olofsson KE, Liu Y, Issazadeh-Navikas S. CD1d-dependent NKT cells play a protective role in acute and chronic arthritis models by ameliorating antigen-specific Th1 responses. J Immunol 2010;185:345–56.
29. Roark CL, French JD, Taylor MA, Bendele AM, Born WK, O'Brien RL. Exacerbation of collagen-induced arthritis by oligoclonal, IL-17-producing γδ T cells. J Immunol 2007;179:5576–83.
30. Peterman GM, Spencer C, Sperling AI, Bluestone JA. Role of γδ T cells in murine collagen-induced arthritis. J Immunol 1993;151: 6546–58.
31. Ito Y, Usui T, Kobayashi S, Iguchi-Hashimoto M, Ito H, Yoshitomi H, et al. Gamma/delta T cells are the predominant source of interleukin-17 in affected joints in collagen-induced arthritis, but not in rheumatoid arthritis. Arthritis Rheum 2009;60:2294–303.
32. Okamoto N, Kanie O, Huang YY, Fujii R, Watanabe H, Shimamura M. Synthetic α-mannosyl ceramide as a potent stimulant for an NKT cell repertoire bearing the invariant Vα19-Jα26 TCR α chain. Chem Biol 2005;12:677–83.
33. Dusseaux M, Martin E, Serriari N, Peguillet I, Premel V, Louis D, et al. Human MAIT cells are xenobiotic-resistant, tissue-targeted, $CD161^{hi}$ IL-17-secreting T cells. Blood 2011;117:1250–9.
34. Shimamura M, Huang YY, Kobayashi M, Goji H. Altered production of immunoregulatory cytokines by invariant Vα19 TCR-bearing cells dependent on the duration and intensity of TCR engagement. Int Immunol 2009;21:179–85.
35. Nagarajan NA, Kronenberg M. Invariant NKT cells amplify the innate immune response to lipopolysaccharide. J Immunol 2007; 178:2706-13.
36. Sutton CE, Lalor SJ, Sweeney CM, Brereton CF, Lavelle EC, Mills KH. Interleukin-1 and IL-23 induce innate IL-17 production from γδ T cells, amplifying Th17 responses and autoimmunity. Immunity 2009;31:331–41.
37. Liu Y, Teige A, Mondoc E, Ibrahim S, Holmdahl R, Issazadeh-Navikas S. Endogenous collagen peptide activation of CD1d-restricted NKT cells ameliorates tissue-specific inflammation in mice. J Clin Invest 2011;121:249–64.
38. Corthay A, Johansson A, Vestberg M, Holmdahl R. Collagen-induced arthritis development requires αβT cells but not γδ T cells: studies with T cell-deficient (TCR mutant) mice. Int Immunol 1999;11:1065–73.
39. Spolski R, Leonard WJ. Interleukin-21: basic biology and implications for cancer and autoimmunity [review]. Annu Rev Immunol 2008;26:57–79.
40. Billerbeck E, Kang YH, Walker L, Lockstone H, Grafmueller S, Fleming V, et al. Analysis of CD161 expression on human CD8+ T cells defines a distinct functional subset with tissue-homing properties. Proc Natl Acad Sci U S A 2010;107:3006–11.
41. Zhu J, Yamane H, Paul WE. Differentiation of effector CD4 T cell populations [review]. Annu Rev Immunol 2010:445–89.
42. Cua DJ, Tato CM. Innate IL-17–producing cells: the sentinels of the immune system [review]. Nat Rev Immunol 2010;10:479–89.
43. Wekerle H. Lessons from multiple sclerosis: models, concepts, observations [review]. Ann Rheum Dis 2008;67 Suppl III:iii56–60.
44. Fletcher JM, Lalor SJ, Sewwney CM, Tubridy N, Mills KH. T cells in multiple sclerosis and experimental autoimmune encephalomyelitis [review]. Clin Exp Immunol 2010;162:1–11.
45. Chiba A, Oki S, Miyamoto K, Hashimoto H, Yamamura T, Miyake S. Suppression of collagen-induced arthritis by natural killer T cell activation with OCH, a sphingosine-truncated analog of α-galactosylceramide. Arthritis Rheum 2004;50:305–13.
46. Coppieters K, Van Beneden K, Jacques P, Dewint P, Vervloet A, Vander Cruyssen B, et al. A single early activation of invariant NK T cells confers long-term protection against collagen-induced arthritis in a ligand-specific manner. J Immunol 2007;179:2300–9.
47. Kaieda S, Tomi C, Oki S, Yamamura T, Miyake S. Activation of invariant natural killer T cells by synthetic glycolipid ligands suppresses autoantibody-induced arthritis. Arthritis Rheum 2007; 56:1836–45.

Experimental Neurology 235 (2012) 436–446

Contents lists available at SciVerse ScienceDirect

Experimental Neurology

journal homepage: www.elsevier.com/locate/yexnr

Review

Molecular network of microRNA targets in Alzheimer's disease brains

Jun-ichi Satoh *

Department of Bioinformatics and Molecular Neuropathology, Meiji Pharmaceutical University, 2-522-1 Noshio, Kiyose, Tokyo 204-8588, Japan

ARTICLE INFO

Article history:
Received 20 April 2011
Revised 24 August 2011
Accepted 4 September 2011
Available online 16 September 2011

Keywords:
Alzheimer's disease
Cell cycle
KEGG
KeyMolnet
MicroRNA
MiRTarBase

ABSTRACT

MicroRNAs (miRNAs) are a group of small noncoding RNAs that regulate translational repression of target mRNAs. The vast majority of presently identified miRNAs are expressed in the brain where they fine-tune the expression of a wide range of target molecules essential for neuronal and glial development, differentiation, proliferation, apoptosis and metabolism. Aberrant expression and dysfunction of brain-enriched miRNAs induce development of neurodegenerative diseases, such as Alzheimer's disease (AD) and Parkinson's disease (PD). Because a single miRNA concurrently downregulates hundreds of target mRNAs, the set of miRNA target genes coregulated by an individual miRNA generally constitutes the biologically integrated network of functionally associated molecules. Recent advances in systems biology enable us to characterize the global molecular network of experimentally validated targets for individual miRNAs by using pathway analysis tools of bioinformatics endowed with comprehensive knowledgebase. This review is conducted to summarize accumulating studies focused on aberrant miRNA expression in AD brains, and to propose the systems biological view that abnormal regulation of cell cycle progression as a result of deregulation of miRNA target networks plays a central role in the pathogenesis of AD.

Contents

Introduction

MicroRNAs (miRNAs) constitute a class of endogenous small noncoding RNAs that mediate posttranscriptional regulation of protein-coding genes by binding mainly to the 3′ untranslated region (3′ UTR) of target mRNAs, leading to translational inhibition, mRNA destabilization or degradation, depending on the degree of sequence complementarity. During their biogenesis, the primary miRNAs (pri-miRNAs) are transcribed from the intra- and inter-genic regions of the genome by RNA polymerase II, and processed by the RNase III enzyme Drosha into pre-miRNAs. After nuclear export, they are processed by RNase III enzyme Dicer into mature miRNAs consisting of approximately 22 nucleotides. Finally, a single-stranded miRNA is loaded onto the RNA-induced silencing complex (RISC), where the seed sequence located at positions 2 to 8 from the 5′ end of the miRNA plays a crucial role in recognition of the target mRNA.

At present, more than one thousand of human miRNAs are registered in miRBase Release 17 (April 2011; www.mirbase.org). A single miRNA capable of binding to numerous target mRNAs concurrently reduces production of hundreds of proteins, whereas the 3′UTR of a single mRNA is often targeted by multiple different miRNAs, providing the complexity of miRNA-regulated gene expression (Filipowicz et al., 2008; Selbach et al., 2008). Consequently, the whole human miRNA system (microRNAome) regulates greater than 60% of all protein-coding genes essential for cellular development, differentiation, proliferation, apoptosis and metabolism (Friedman et al., 2009). Approximately 70% of presently identified miRNAs are expressed in the brain in a spatially and temporally controlled manner, where they fine-tune diverse neuronal and glial functions (Fineberg et al., 2009). Actually, aberrant expression and dysfunction of brain-enriched miRNAs induce development of neurodegenerative diseases, such as Alzheimer's disease (AD) and Parkinson's disease

* Corresponding author. Fax: +81 42 495 8678.
E-mail address: satoj@my-pharm.ac.jp.

0014-4886/$ – see front matter © 2011 Elsevier Inc. All rights reserved.
doi:10.1016/j.expneurol.2011.09.003

Table 1
Aberrant expression of miRNAs in AD brains.

Authors and years	Patients and brain regions	Methods for miRNA expression profiling	Aberrantly expressed miRNAs	Upregulation or downregulation	Target mRNAs characterized	Target prediction and validation	Possible pathological implications
Lukiw (2007)	5 AD patients and 5 age-matched controls; the hippocampus	Northern blot	miR-9, miR-128	Up	ND	ND	General neuropathology of AD
Lukiw et al. (2008)	23 AD patients and 23 age-matched controls; the hippocampus and the superior temporal lobe neocortex	Microarray, northern blot	miR-146a	Up	CFH	ND; knockdown of miR-146a	Sustained inflammatory responses
Wang et al. (2008)	6 AD and 6 MCI patients and 11 non-demented controls; the temporal cortex	Microarray, northern blot, ISH	miR-107	Down	BACE1	miRanda, TargetScan, PicTar; luciferase reporter assay	Increased production of Ab
Hébert et al. (2008)	5 AD patients and 5 age-matched controls; the anterior temporal cortex	Microarray, qRT-PCR	miR-29a/b-1	Down	BACE1	miRanda, TargetScan, Pictar, miRBase; luciferase reporter assay	Increased production of Ab
			miR-15a, miR-9, miR-19b	Down	BACE1	miRanda, TargetScan, Pictar, miRBase; not validated	
			let-7i, miR-15a, miR-101, miR-106b	Down	APP	miRanda, TargetScan, Pictar, miRBase; not validated	
			miR-22, miR-26b, miR-93, miR-181c, miR-210, miR-363	Down	ND	ND	
			miR-197, miR-511, miR-320	Up	ND	ND	
Cogswell et al. (2008)	15 AD patients and 12 non-demented controls; the cerebellum	qRT-PCR	miR-27a, miR-27b, miR-34a, miR-100, miR-125b, miR-381, miR-422a	Up	ND	miRanda, RNAhybrid; not validated	General neuropathology of AD
			miR-9, miR-98, miR-132, miR-146b, miR-212, miR-425	Down	ARHGAP32 for miR-132		
	15 AD patients and 12 *non-demented controls*; the hippocampus		miR-26a, miR-27a, miR-27b, *miR-30e-5p, miR-34a, miR-92,* miR-125b, miR-145, miR-200c, miR-381, miR-422a, miR-423	Up	ND		
			miR-9, miR-30c, miR-132, miR-146b, miR-210, miR-212, miR-425	Down	ARHGAP32 for miR-132		
	15 AD patients and 12 non-demented controls; the medial frontal gyrus		miR-27a, miR-27b, miR-29a, miR-29b, miR-30c, miR-30e-5p, miR-34a, miR-92, miR-100, miR-125b, miR-145, miR-148a, miR-381, miR-422a, miR-423	Up	ND		
			miR-9, miR-26a, miR-132, miR-146b, miR-200c, miR-210, miR-212, miR-425	Down	ARHGAP32 for miR-132		
Hébert et al. (2009)	19 AD patients and 11 non-demented controls; the anterior temporal cortex	qRT-PCR	miR-106b	Down	APP	miRanda, TargetScan, Pictar, miRBase; luciferase reporter assay	Increased production of Ab
Sethi and Lukiw (2009)	6 AD and 13 non-AD patients and 6 controls; the temporal lobe cortex	Microarray, northern blot	miR-9, miR-125b, miR-146a	Up	ND	ND	General neuropathology of AD
Nunez-Iglesias et al. (2010)	5 AD patients and 5 age-matched controls; the parietal lobe cortex	Microarray	miR-18b, miR-34c, miR-615, miR-629, miR-637, miR-657, miR-661, mir-09369, mir-15903, mir-44691	Nd	positively correlated with target mRNAs	miRanda, TargetScan, PicTar; not validated	General neuropathology of AD
			miR-211, miR-216, miR-325, miR-506, miR-515-3p, miR-612, *miR-768-3p, mir-06164,* mir-32339, mir-45496	Nd	negatively correlated with target mRNAs	miRanda, TargetScan, PicTar; not validated	

(continued on next page)

Table 1 (*continued*)

Authors and years	Patients and brain regions	Methods for miRNA expression profiling	Aberrantly expressed miRNAs	Upregulation or downregulation	Target mRNAs characterized	Target prediction and validation	Possible pathological implications
Shioya et al. (2010)	7 AD patients and 4 non-neurological controls; the frontal lobe	qRT-PCR	miR-29a	Down	NAV3	TargetScan, Pictar, miRBase; luciferase reporter assay	A putative compensatory mechanism against neurodegenerative events
Hébert et al. (2010)	8 AD patients and 10 non-demented patients; the anterior temporal cortex	qRT-PCR	miR-15a	Down	ERK1	TargetScan, miRanda; overexpression or knockdown of miR-15a, luciferase reporter assay	Hyperphosphorylation of tau
Cui et al. (2010)	36 AD patients and 30 age-matched controls; the hippocampus and the superior temporal lobe neocortex	Microarray, northern blot	miR-146a	Up	IRAK1	miRBase; knockdown of miR-146a	Sustained inflammatory responses
Faghihi et al. (2010)	35 AD patients and 35 normal elderly controls; the entorhinal cortex and the hippocampus	qRT-PCR	miR-485-5p	Down	BACE1	miRanda; luciferase reporter assay	increased production of Ab
Smith et al. (2011)	11 AD patients and 11 non-demented patients; the anterior temporal cortex	qRT-PCR	miR-124	Down	PTBP1	known target previously validated by luciferase reporter assay	Aberrant APP mRNA alternative splicing
Wang et al. (2011)	10 elderly females with various pathological stages of AD; the gray matter and the white matter of the superior and middle temporal cortex	Microarray, northern blot	miR-519e, miR-574-5p, miR-498, miR-518a-5p/miR-527, miR-525-5p, miR-300, miR-576-3p, miR-583, miR-146b-3p, miR-490-3p, miR-549, miR-516a-5p, miR-510, miR-184, miR-516b, miR-298, miR-214, miR-198, miR-451, miR-144, miR-424, let-7e miR-509-5p, miR-574-3p, miR-576-5p, miR-302e, miR-220b, miR-208a, miR-215 miR-485-3p, miR-381, miR-124, miR-34a, miR-129-5p, miR-29a, miR-143, miR-136, miR-145, miR-138, miR-129-3p, miR-128, miR-379, miR-299-5p, miR-218, miR-149, miR-135a, miR-7, miR-126, miR-411, miR-335, miR-9, miR-378, miR-488, miR-432,	Up in the gray matter (group A) Up in the white matter (group B) Down in the gray matter (group C)	ND	ND	General neuropathology of AD

miR-127-5p, miR-127-3p, miR-491-5p, miR-376c, miR-377, miR-95, miR-222, miR-29b, miR-329, miR-495, miR-551b, miR-195, miR-125b, miR-30b, miR-221, miR-139-5p, miR-487a, miR-487b, miR-107, miR-146b-5p, miR-29c, miR-30a, miR-582-5p, miR-103, miR-342-3p, miR-331-3p, miR-30c, miR-30d, miR-382, miR-22, miR-125a-5p	
miR-491-3p, miR-423-5p, miR-34b, miR-422a, miR-34c-5p, miR-584, miR-219-5p, miR-338-3p, miR-219-2-3p, miR-338-5p, miR-181a, miR-181b, let-7b, miR-151-3p, miR-197, miR-19a, miR-20a, miR-17, miR-106a, miR-32, miR-340, miR-19b, miR-21, miR-151-5p, miR-194, let-7c, miR-330-3p, miR-27b, miR-93, miR-15a, miR-339-5p, miR-193b, miR-106b, miR-16, miR-23b, miR-15b, miR-320d, miR-320b, miR-320c, miR-320a, miR-557, miR-33a, let-7a, miR-374b, miR-140-3p, miR-374a, miR-24, miR-140-5p, miR-26a, miR-513a-5p, miR-212, miR-142-5p, miR-142-3p, miR-26b, miR-520d-5p, miR-193a-3p, miR-92b, miR-330-5p, miR-186, let-7f, miR-223, miR-412, miR-185, miR-148b, miR-101, miR-99b, miR-27a, miR-589, let-7i, miR-361-3p, miR-361-5p, miR-423-3p, miR-190, miR-301a, miR-365, miR-23a, miR-363, miR-326	Down in the white matter (group D)
miR-425, miR-191, miR-519d, let-7 g, miR-98, miR-99a, miR-30e	Down in the gray matter (group E)

The table is modified from that of the recent review article with permission of reproduction (Satoh, 2010). Abbreviations: AD, Alzheimer disease; MCI, mild cognitive impairment; qRT-PCR, quantitative RT-PCR; ISH, in situ hybridization; BACE1, beta-site APP-cleaving enzyme 1; APP, amyloid precursor protein; Ab, amyloid-beta; CFH, complement factor H; NAV3, neuron navigator 3; ERK1, extracellular signal-regulated kinase 1; ARHGAP32, Rho GTPase activating protein 32 (p250GAP); IRAK1, IL-1 receptor-associated kinase-1; PTBP1, polypyrimidine tract binding protein 1; and ND, not determined.

(PD) (Harraz et al., 2011; Kocerha et al., 2009; Maes et al., 2009; Nelson et al., 2008).

Recent advances in systems biology have made major breakthroughs by illustrating the cell-wide map of complex molecular interactions with the aid of the literature-based knowledgebase of molecular pathways (Viswanathan et al., 2008). The logically arranged molecular networks construct the whole system characterized by robustness that maintains the proper function of the system in the face of genetic and environmental perturbations (Kitano, 2007). In the scale-free molecular network, targeted disruption of several critical components designated hubs, on which the biologically important molecular interactions concentrate, efficiently disturbs the whole cellular function by destabilizing the network (Albert et al., 2000). From the point of view of the molecular network constructed by target genes for a particular miRNA, the identification and characterization of the hub would help us to understand biological and pathological roles of the individual miRNA. By combining the application of the miRNA target prediction program TargetScan and the Human Protein Reference Database (HPRD), a recent study investigated the global human microRNA-regulated protein–protein interaction (PPI) network (Hsu et al., 2008). Importantly, individual miRNAs often target the hub itself within the PPI network.

AD is the most common cause of dementia worldwide, affecting the elderly population, characterized by the hallmark pathology of amyloid-β (Aβ) deposition, neurofibrillary tangle (NFT) formation, and extensive neuronal degeneration in the brain. Aβ is derived from the sequential cleavage of amyloid precursor protein (APP) by beta-site APP-cleaving enzyme 1 (BACE1) and the γ-secretase complex. Although the precise pathological mechanisms underlying AD remain largely unknown, accumulating evidence indicates that aberrant regulation of miRNA-dependent gene expression is closely associated with molecular events responsible for Aβ production, NFT formation, and neurodegeneration (Hébert et al., 2008, 2010; Wang et al., 2008, 2011). The aim of the present study is to review recent studies focused on aberrant miRNA expression in AD brains, and to propose the systems biological view that deregulation of miRNA target networks plays a central role in the pathogenesis of AD.

Aberrant miRNA expression in AD brains

Increasing evidence indicates that deregulation of miRNA expression plays a key role in AD pathogenesis, as a recent review indicated (Table 1 modified from Satoh, 2010). The pioneering work identified upregulated expression of miR-9 and miR-128 in the hippocampus of AD brains by using a nylon membrane-bound DNA array (Lukiw, 2007). More recently, the same group showed that the levels of expression of miR-146a are elevated in the hippocampus and the superior temporal cortex of AD patients (Lukiw et al., 2008). Importantly, nuclear factor-kappa B (NF-κB), a transcription factor indispensable for diverse immune responses, regulates the expression of miR-146a that targets complement factor H (CFH) and IL-1 receptor-associated kinase-1 (IRAK1), leading to sustained inflammation in AD brains where the expression of NF-κB is also upregulated (Cui et al., 2010; Lukiw et al., 2008). Furthermore, they clarified the limited stability of brain-enriched miRNAs composed of a high content of AU and UA dinucleotides (Sethi and Lukiw, 2009).

A different group showed that miR-107 targets BACE1, a rate-limiting enzyme for Aβ production (Wang et al., 2008). By analyzing a miRNA microarray, they found that miR-107 levels are substantially reduced in the temporal cortex not only of AD but also of the patients affected with mild cognitive impairment (MCI), indicating that downregulation of miR-107 begins at the very early stage of AD. More recently, they validated a negative correlation between miR-107 levels and the amounts of neuritic plaques and NFTs in the temporal cortex of AD patients by quantitative RT-PCR (qRT-PCR) (Nelson and Wang, 2010). The levels of miR-107 and miR-103, both of which target the actin-binding protein cofilin, are reduced in the brains of Tg19959 mice overexpressing human APP carrying the KM670/671NL and V717F familial AD mutations (Yao et al., 2010). These observations are responsible for formation of rod-like aggregates of cofilin in brains of a transgenic mouse model of AD.

By using a miRNA microarray, a previous study identified reduced expression of the miR-29a/b-1 cluster, inversely correlated with BACE1 protein levels, in the anterior temporal cortex of AD patients (Hébert et al., 2008). The miRNA target database search predicted the presence of binding sites in the human BACE1 mRNA 3′UTR for miR-9, 15a, 19b, and 29a/b-1 and in the human APP mRNA 3′UTR for let-7, miR-15a, 101, and 106b, all of which are downregulated in AD brains. Actually, the introduction of pre-miR-29 reduces secretion of Aβ from HEK293 cells stably expressing the APP Swedish (APPswe) mutation (Hébert et al., 2008). Later, they identified reduced expression of miR-106b that targets APP in the anterior temporal cortex of AD patients (Hébert et al., 2009).

The levels of miR-298 and miR-328, both of which target mouse BACE1, are reduced in the hippocampus of aged APPswe/PS1(A246E) transgenic mice (Boissonneault et al., 2009). In contrast, the levels of a noncoding BACE1-antisense (BACE1-AS) RNA that enhances BACE1 mRNA stability are elevated in the brains of Tg19959 APP transgenic mice (Faghihi et al., 2008). BACE1-AS masks the miR-485-5p binding site located within the open-reading frame of BACE1 mRNA, and thereby inhibits miR-485-5p-mediated repression of BACE1 mRNA translation (Faghihi et al., 2010). Actually, the levels of expression of miR-485-5p are reduced but those of BACE1-AS are elevated in the entorhinal cortex and the hippocampus of AD patients. In cultured rat hippocampal neurons, a brain-enriched microRNA miR-101 acts as a negative regulator of APP expression by binding to the APP 3′UTR (Vilardo et al., 2010).

All of these observations suggest the concept that abnormal repression of a battery of miRNAs accelerates Aβ production via overexpression of BACE1, the enzyme and/or APP, the substrate in AD brains. However, the genetic variability of miRNA-binding sites in both BACE1 and APP mRNA 3′UTRs does not confer a risk factor for development of AD (Bettens et al., 2009). It sounds reasonable, because miRNAs in general induce translational inhibition without requiring the perfect match of binding sequences in target mRNAs. It is worthy to note that a neuron-specific microRNA miR-124, downregulated in the anterior temporal cortex of AD brains, targets polypyrimidine tract binding protein 1 (PTBP1), a global repressor of alternative pre-mRNA splicing (Smith et al., 2011). Upregulation of PTBP1 induces the inclusion of APP exons 7 and 8, suggesting a novel role of miRNAs in neuronal splicing regulation of APP.

By qRT-PCR and luciferase reporter assay, we found that miR-29a, whose levels are decreased in the frontal cortex of AD brains, targets neuron navigator 3 (NAV3) (Shioya et al., 2010). NAV3 immunoreactivity was greatly enhanced in NFT-bearing pyramidal neurons in the cerebral cortex of AD brains. Although the precise biological function of the human NAV3 protein remains unknown, the *Caenorhabditis elegans* homolog regulates axon guidance (Maes et al., 2002), suggesting that our findings reflect a neuronal compensatory response against NFT-generating neurodegenerative events. The conditional deletion of Dicer, a master regulator of miRNA processing, induces neurodegeneration accompanied by hyperphosphorylation of tau in the adult mouse forebrain and the hippocampus (Hébert et al., 2010). They identified extracellular signal-regulated kinase 1 (ERK1) regulated by the miR-15 family as a candidate kinase responsible for tau phosphorylation. The levels of miR-15a are substantially reduced in AD brains.

By qRT-PCR, a previous study characterized miRNA expression profiles of the brain and cerebrospinal fluid (CSF) samples isolated from AD patients and non-demented controls (Cogswell et al., 2008). Among a panel of miRNAs either upregulated or downregulated in the hippocampus, the medial frontal cortex, and the cerebellum of AD patients, they identified a close relationship between upregulated miRNAs and metabolic pathways, including insulin signaling, glycolysis, and

glycogen metabolism. Furthermore, they found that the levels of all miR-30 family members are elevated in CSF samples of AD patients. Because circulating miRNAs in the plasma serve as a biomarker for diagnosis and prediction of prognosis of human cancers (Mitchell et al., 2008), the identification of AD-specific miRNAs in the serum and the CSF would be a worthwhile project in the future.

By combining microarray-based miRNA expression profiling and genome-wide transcriptome analysis of the brains of AD patients and age-matched controls, a recent study showed that the levels of several miRNAs are not only negatively but also positively correlated with those of potential target mRNAs (Nunez-Iglesias et al., 2010). The expression of miR-211 shows a negative correlation with mRNA levels of BACE1, RAB43, LMNA, MAP2K7, and TADA2L, whereas the expression of mir-44691 exhibits a positive correlation with mRNA levels of CYR61, CASR, POU3F2, GGPR68, DPF3, STK38, and BCL2L2 in AD brains. Although a previous study showed that certain miRNAs exceptionally activate transcription and translation of targets (Vasudevan et al., 2007), the direct interaction between mir-44691 and their targets requires further investigation and validation.

Thus, different studies identified aberrant expression of distinct miRNAs in AD brains. This variability is mostly attributable to disease-specific and nonspecific interindividual differences, including differences in age, sex, genetic background, the brain region, the pathological stage, and the postmortem interval (PMI), because most studies include fairy limited numbers of patients' samples and controls, which are often complicated by variable confounding factors (Table 1). Importantly, distinct populations of neurons in different cerebral cortical layers express a discrete set of miRNAs in the human transentorhinal cortex (Nelson et al., 2010).

MicroRNA target networks suggest the involvement of deregulation of cell cycle progression in AD pathogenesis

Because a single miRNA concurrently downregulates hundreds of target mRNAs, the set of miRNA target genes coregulated by an individual miRNA generally constitutes the biologically integrated network of functionally associated molecules (Hsu et al., 2008; Satoh and Tabunoki, 2011). Even small changes in the expression level of a single miRNA could affect a wide range of signaling pathways involved in diverse biological functions. From this point of view, the characterization of a global picture of miRNA target networks would promote us to understand miRNA-mediated molecular mechanisms underlying AD.

To identify biologically relevant molecular networks from the large-scale data, we could analyze them by using a battery of pathway analysis tools of bioinformatics endowed with comprehensive knowledgebase, such as Kyoto Encyclopedia of Genes and Genomes (KEGG) (Kanehisa et al., 2010; www.kegg.jp), Ingenuity Pathways Analysis (IPA) (Ingenuity Systems; www.ingenuity.com), and KeyMolnet (Institute of Medicinal Molecular Design; www.immd.co.jp). KEGG is a public database, while both IPA and KeyMolnet are commercial ones. KEGG includes manually curated reference pathways that cover a wide range of metabolic, genetic, environmental, and cellular processes, and human diseases. Currently, KEGG contains 134,511 distinct pathways generated from 391 reference pathways.

IPA is a knowledgebase that contains approximately 2,270,000 biological and chemical interactions and functional annotations with definite scientific evidence, curated by expert biologists. By uploading the list of Gene IDs and expression values, the network-generation algorithm identifies focused genes integrated in a global molecular network. IPA calculates the score p-value that reflects the statistical significance of association between the genes and the networks by the Fisher's exact test.

KeyMolnet contains knowledge-based contents on 131,000 relationships among human genes and proteins, small molecules, diseases, pathways and drugs, curated by expert biologists (Satoh et al., 2009). They are categorized into the core contents collected from selected review articles with the highest reliability or the secondary contents

Table 2
Gene ontology terms of target genes for miRNAs downregulated in AD brains.

Rank	GO term	The number of genes in the term	Bonferroni corrected p-value
1	GO:0042127 – regulation of cell proliferation	126	3.37E-25
2	GO:0043067 – regulation of programmed cell death	119	4.03E-20
3	GO:0010941 – regulation of cell death	119	5.55E-20
4	GO:0042981 – regulation of apoptosis	117	1.88E-19
5	GO:0043069 – negative regulation of programmed cell death	69	1.88E-16
6	GO:0051094 – positive regulation of developmental process	60	2.01E-16
7	GO:0060548 – negative regulation of cell death	69	2.20E-16
8	GO:0045597 – positive regulation of cell differentiation	54	2.80E-16
9	GO:0043066 – negative regulation of apoptosis	68	3.75E-16
10	GO:0010604 – positive regulation of macromolecule metabolic process	114	1.00E-15
11	GO:0008284 – positive regulation of cell proliferation	73	2.13E-15
12	GO:0051726 – regulation of cell cycle	61	4.12E-13
13	GO:0012501 – programmed cell death	87	8.24E-13
14	GO:0031328 – positive regulation of cellular biosynthetic process	93	1.24E-12
15	GO:0006357 – regulation of transcription from RNA polymerase II promoter	96	2.47E-12
16	GO:0009891 – positive regulation of biosynthetic process	93	3.71E-12
17	GO:0010033 – response to organic substance	95	4.53E-12
18	GO:0051174 – regulation of phosphorus metabolic process	74	5.36E-12
19	GO:0019220 – regulation of phosphate metabolic process	74	5.36E-12
20	GO:0042325 – regulation of phosphorylation	72	7.00E-12

The list of 852 target genes for the set of miRNAs downregulated in AD brains was imported into the Functional Annotation tool of DAVID. The top 20 GO terms showing a significant association with target genes are listed with rank, GO term, the number of genes in the term, and p-value following Bonferroni correction.

Table 3
KEGG pathways of target genes for miRNAs downregulated in AD brains.

Rank	KEGG pathway	The number of genes in the pathway	Bonferroni corrected p-value
1	hsa05200:Pathways in cancer	81	3.16E-21
2	hsa05220:Chronic myeloid leukemia	32	3.77E-14
3	hsa05212:Pancreatic cancer	30	7.55E-13
4	hsa05219:Bladder cancer	23	2.00E-12
5	hsa05215:Prostate cancer	32	9.63E-12
6	hsa05222:Small cell lung cancer	28	3.81E-09
7	hsa05210:Colorectal cancer	27	2.35E-08
8	hsa05223:Non-small cell lung cancer	21	9.28E-08
9	hsa05218:Melanoma	24	1.02E-07
10	hsa04110:Cell cycle	32	1.92E-07
11	hsa04510:Focal adhesion	42	2.35E-07
12	hsa04012:ErbB signaling pathway	26	3.12E-07
13	hsa05214:Glioma	22	3.23E-07
14	hsa05213:Endometrial cancer	20	3.32E-07
15	hsa05211:Renal cell carcinoma	21	1.52E-05
16	hsa04115:p53 signaling pathway	20	4.75E-05
17	hsa05221:Acute myeloid leukemia	18	9.63E-05
18	hsa04010:MAPK signaling pathway	43	3.40E-04
19	hsa04914:Progesterone-mediated oocyte maturation	21	5.61E-04
20	hsa04350:TGF-beta signaling pathway	21	6.79E-04

The list of 852 target genes for the set of miRNAs downregulated in AD brains was imported into the Functional Annotation tool of DAVID. The top 20 KEGG pathways showing a significant association with target genes are listed with rank, KEGG pathway, the number of genes in the pathway, and p-value following Bonferroni correction. The molecular pathway entitled "hsa04110:Cell cycle" (Rank 10) is illustrated in Fig. 1.

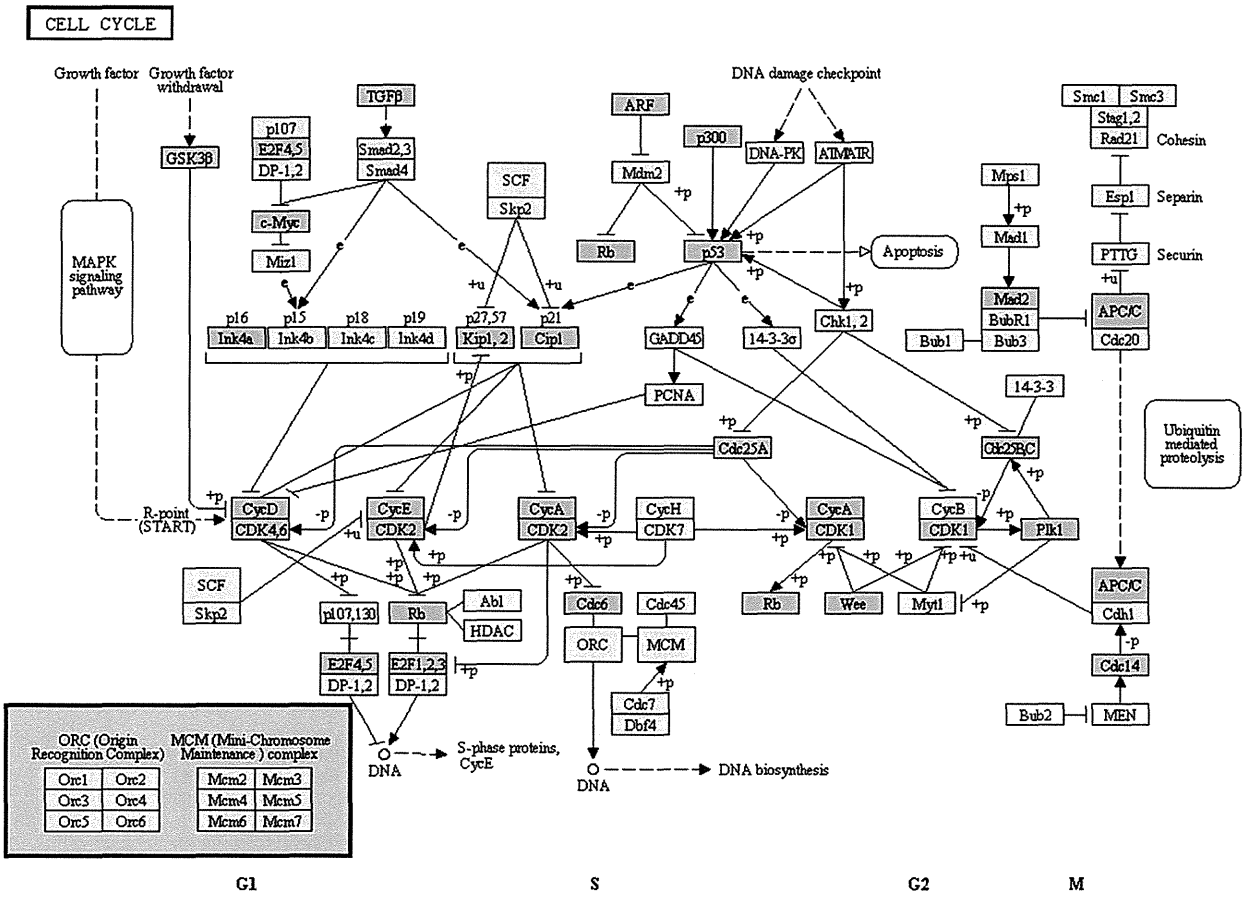

Fig. 1. Target genes for miRNAs downregulated in AD brains are located in the cell cycle pathway of KEGG. The list of 852 target genes for the set of miRNAs downregulated in AD brains (Supplementary Table 1) was imported into the Functional Annotation tool of DAVID. Among the top 20 KEGG pathways showing a significant association with target genes, the molecular pathway entitled "hsa04110:Cell cycle" (Rank 10 in Table 3) is illustrated. Target genes highlighted by pink are potentially upregulated in AD brains.

extracted from abstracts of PubMed and HPRD. By uploading the list of Gene IDs, KeyMolnet automatically provides corresponding molecules and a minimum set of intervening molecules as a node on networks. The "neighboring" network-search algorithm selected one or more molecules as starting points to generate the network of all kinds of molecular interactions around starting molecules, including direct activation/inactivation, transcriptional activation/repression, and the complex formation within the designated number of paths from starting points. The generated network was compared side by side with 443 human canonical pathways of the KeyMolnet library. The algorithm counting the number of overlapping molecular relations between the extracted network and the canonical pathway makes it possible to identify the canonical pathway showing the most significant contribution to the extracted network. The significance in the similarity between both is scored following the formula, where O = the number of overlapping molecular relations between the extracted network and the canonical pathway, V = the number of molecular relations located in the extracted network, C = the number of molecular relations located in the canonical pathway, T = the number of total molecular relations, and the X = the sigma variable that defines coincidence.

$$\text{Score} = -\log_2(\text{Score(p)}) \qquad \text{Score(p)} = \sum_{x=0}^{\text{Min(C,V)}} f(x) \qquad f(x) = {}_{C}C_{X} \cdot {}_{T-C}C_{V-X} / {}_{T}C_{V}.$$

In the present study, we attempted to characterize the networks of target genes for a battery of miRNAs aberrantly expressed in AD brains. For this purpose, we have focused on the currently available most comprehensive dataset of miRNA expression profiling of AD brains (Wang et al., 2011) (Table 1). This includes expression profiles of miRNAs isolated separately from the gray matter and the white matter of the superior and middle temporal cerebral cortex. All samples were taken within 4 h at PMI and processed for the rigid control of RNA quality. The samples were derived from control subjects with no AD pathology and the patients with the early AD pathology, evaluated by the density of diffuse plaques, neuritic plaques, and NFTs. Hierarchical clustering of expression profiles categorized AD-relevant 171 miRNAs into five groups tentatively named A to E, presenting with similar expression patterns within the group, either upregulated or downregulated in the gray matter or in the white matter of AD brains (Wang et al., 2011) (Table 1). Because the white matter is enriched in neuronal axons in which certain miRNAs are transported (Schratt et al., 2006), the white matter-enriched fraction does not exclude the inclusion of neuron-specific miRNAs. For simplicity, we combined the data of the white matter and the gray matter fractions, and separated them into two categories, such as the set of upregulated miRNAs consisting of groups A and B and the set of downregulated miRNAs consisting of groups C, D, and E.

Recently, various bioinformatics programs armed with distinct algorithms have been established for the in silico prediction of miRNA

Table 4
IPA functional networks of target genes for miRNAs downregulated in AD brains.

Rank	IPA functional network	Molecules in the network	Fisher's test p-value
1	Cancer, dermatological diseases and conditions, cellular growth and proliferation	Ap1, BCL2, CAV1, CEBPA, CEP63, COMMD9, CTGF, ETS1, FGF2, GLI1, HRAS, Ige, JUN, KRAS, NFKB1, NIPAL2, Nos, OSBPL8, P38 MAPK, PAPSS2, PLAG1, PTGFRN, PTGS2, PXDN, SERBP1, SIGMAR1, SOX9, SP1, SP3, SPP1, SQSTM1, VDR, VEGFA, VIM, WT1	1.00E-43
2	Organ development, cellular development, nervous system development and function	ACTR8, ACVR1, ACVR1B, ADSS, Alp, ANKRD27, BMP, BMP7, BMPR2, BMPR1B, COL1A2, CSHL1, CTDSP1, CTDSP2, DLL1, GSK3B, HES1, ID2, ID3, IGF2BP1, KLF4, MIR24 (human), Notch, NOTCH1, NOTCH2, Pro-inflammatory Cytokine, RAB21, Smad, SMAD1, SMAD5, SOX2, TGFBR1, TGFBR2, UHMK1, ZBED3	1.00E-38
3	Gene expression, cell cycle, DNA replication, recombination, and repair	ASXL2, BMI1, BTG2, CBX7, CDCA4, CDK2-CyclinE, DHFR, DNA (cytosine-5-)-methyltransferase, DNMT1, DNMT3A, DNMT3B, E2F2, E2F3, E2F5, E2F6, ERK, EZH2, Gap, HELLS, JARID2, MIR101, MIR125B (human), MIR26A (human), MYT1, PHB, PHF19, RING1, SGPL1, SNAI2, SPRED1, TDG, Thymidine Kinase, TYMS, UHRF1, ZNF238	1.00E-34
4	Cell cycle, connective tissue development and function, cellular growth and proliferation	ARID4B, ARL2, AURKB, BRCA1, CA12, CCDC99, CCNT2, CDCA7L, CDKN2A, DKK1, DRAM1, E2F1, Ep300/Pcaf, ERH, EYA4, FAM3C, GTF2H1, Histone h4, Holo RNA polymerase II, P-TEFb, PERP, PRMT5, Rb, RNA polymerase II, RPA, RRP8, SIRT1, TAF9B, TARBP1, TMED2, TMED7, TMED10, TMEM43, TP53, TP53INP1	1.00E-33
5	Lipid metabolism, molecular transport, small molecule biochemistry	26s Proteasome, Alpha tubulin, ARIH2, ATXN1, CDC34, CDKAL1, FADS2, HARS, HMG CoA synthase, Ikb, IKK (complex), LASS2, MAN2A1, MAPK1IP1L, MDM4, NOVA1, ODZ2, PECI, PFK, PTEN, RAD23B, SLC25A1, SLC25A22, SNCA, SOX4, SRSF10, TUBB6, UBE2, Ube3, UBE2I, UBE2Q1, UBE2S, UBE2V1, Ubiquitin, UGP2	1.00E-31
6	Lipid metabolism, small molecule biochemistry, cell signaling	ACAA2, acetyl-CoA C-acyltransferase, ANXA8/ANXA8L1, Arginase, BACE1, BNIP3L, CASP6, CASP3/6/7, Cytokeratin, Fgfr, FMOD, FNDC3B, HADH, HADHB, Hspg, IMPDH1, Lamin, LMNB1, MBNL2, Mediator, Mhc class ii, MPHOSPH9, MTRR, NAT6, NUCB1, PGRMC1, PGRMC2, PNP, RBMS1, RPS7, SLC35A1, Tenascin, TGFB1, UGDH, VPS39	1.00E-30
7	Cell cycle, cell death, cancer	ABHD5, ADIPOR2, AP2A1, APC, APP, CDKN1A, CLDND1, ELMOD2, EP300, ERBB2, GLCCI1, Hemoglobin, HIF1A, HISTONE, Histone h3, HNRNPK, IL1, Insulin, LAMB3, LRRC8C, MAN1A1, MYC, Ndpk, NR3C1, PPARA, PPARG, RAB34, RAD51C, RB1, RELA, ROCK2, SLC38A1, SLC7A11, TNFRSF21, UTP15	1.00E-30
8	Cell-to-cell signaling and interaction, cellular growth and proliferation, connective tissue development and function	ATP2A2, BRAP, CCND1, CCND2, CCND3, CDCA7, CENPJ, CTNNBIP1, Cyclin D1/cdk4, EIF4A, EIF4A1, EIF4E, Eif4ebp, EIF4EBP1, Eif4g, Gm-csf, IDH1, IGF2, IGF2R, JAK2, KAT2B, LIF, MTPN, NR4A2, p70 S6k, Pdgf (complex), PDGF BB, PMS1, SKAP2, STAT, STAT5A, STAT5a/b, TGFB3, TUSC2, UAP1	1.00E-29
9	Cellular growth and proliferation, tumor morphology, cellular development	Adaptor protein 1, AFF1, AP1M2, Camk, CAMK2G, Creb, CREB1, DNAJ, DNAJB4, DNAJB11, DNAJC1, DNAJC27, Gi-coupled receptor, Glutathione peroxidase, GSTM4, Hdac, HDAC4, HLA-G, HOXA11, HSP, Hsp70, Hsp90, Hsp22/Hsp40/Hsp90, HSP90B1, HSPA1A/HSPA1B, HSPB6, INO80C, MHC Class II (complex), MLL, MLLT1, OPRM1, PDHA2, SLC16A1, SOD2, TFRC	1.00E-26
10	Cell death, cellular growth and proliferation, connective tissue development and function	BIRC3, CASP3, CASP7, Caspase, CCL2, CCL4, CD8, CDC6, CHEMOKINE, COX4I1, DFF, DFFA, DFFB, DR4/5, DUB, HERC6, Hsp27, IFIT5, Ifn gamma, IL-1R, IL1RN, Interferon alpha, LDL, MCL1, NAIP, NEDD4, PANX1, PDCD6IP, PLSCR3, RFFL, TNFRSF10B, TNFSF10, USP18, USP48, USP49	1.00E-26

The list of 852 target genes for the set of miRNAs downregulated in AD brains was uploaded into IPA. The top 10 functional networks showing a significant association with target genes are listed with rank, IPA functional network, molecules in the network, and p-value by the Fisher's Exact test. The molecular network entitled "Cell cycle, connective tissue development and function, cellular growth and proliferation" (Rank 4) is illustrated in Fig. 2.

target genes, such as TargetScan 5.1 (www.targetscan.org), PicTar (pictar.mdc-berlin.de), miRanda (www.microrna.org), MicroCosm (www.ebi.ac.uk/enright-srv/microcosm/htdocs/targets/v5), and DianamicroT 3.0 (diana.cslab.ece.ntua.gr/microT). However, the miRNA target prediction by these programs is often hampered by detection of numerous false positive targets. To avoid this problem, we explored the targets for AD-relevant 171 miRNAs of Wang's dataset by using the miRTarBase (mirtarbase.mbc.nctu.edu.tw), the recently established largest collection of more than 3500 manually curated miRNA-target interactions from 985 articles, all of which are experimentally validated by luciferase reporter assay, western blot, qRT-PCR, microarray experiments with overexpression or knockdown of miRNAs, or pulsed stable isotope labeling with amino acids in culture (pSILAC) experiments (Hsu et al., 2011) (Supplementary Tables 1 and 2).

Although experimentally validated targets represent a source of reliable candidates, it is worthless when they are not expressed in the human brain. Therefore, we verified the expression of target genes in the human brain at mRNA levels by analyzing them on UniGene (www.ncbi.nlm.nih.gov/unigene), an organized view of the transcriptome that semi-quantitatively exhibits the expression sequence tag (EST) profile as the number of transcripts per million (TPM). After omitting the genes undetectable in the human brain, we identified 852 non-redundant target genes for the set of miRNAs downregulated in AD brains (Supplementary Table 1). We also found 39 non-redundant target genes for the set of miRNAs upregulated in AD brains (Supplementary Table 2). Since the former greatly outnumbered the latter, thereafter, we have focused on molecular networks of 852 theoretically upregulated targets for the set of downregulated miRNAs in AD brains.

Next, we investigated molecular networks of 852 genes by searching them on the Database for Annotation, Visualization and Integrated Discovery (DAVID) (david.abcc.ncifcrf.gov), which automatically outputs the results from KEGG pathway analysis (Huang et al., 2009). When Entrez Gene IDs of 852 genes were imported into the

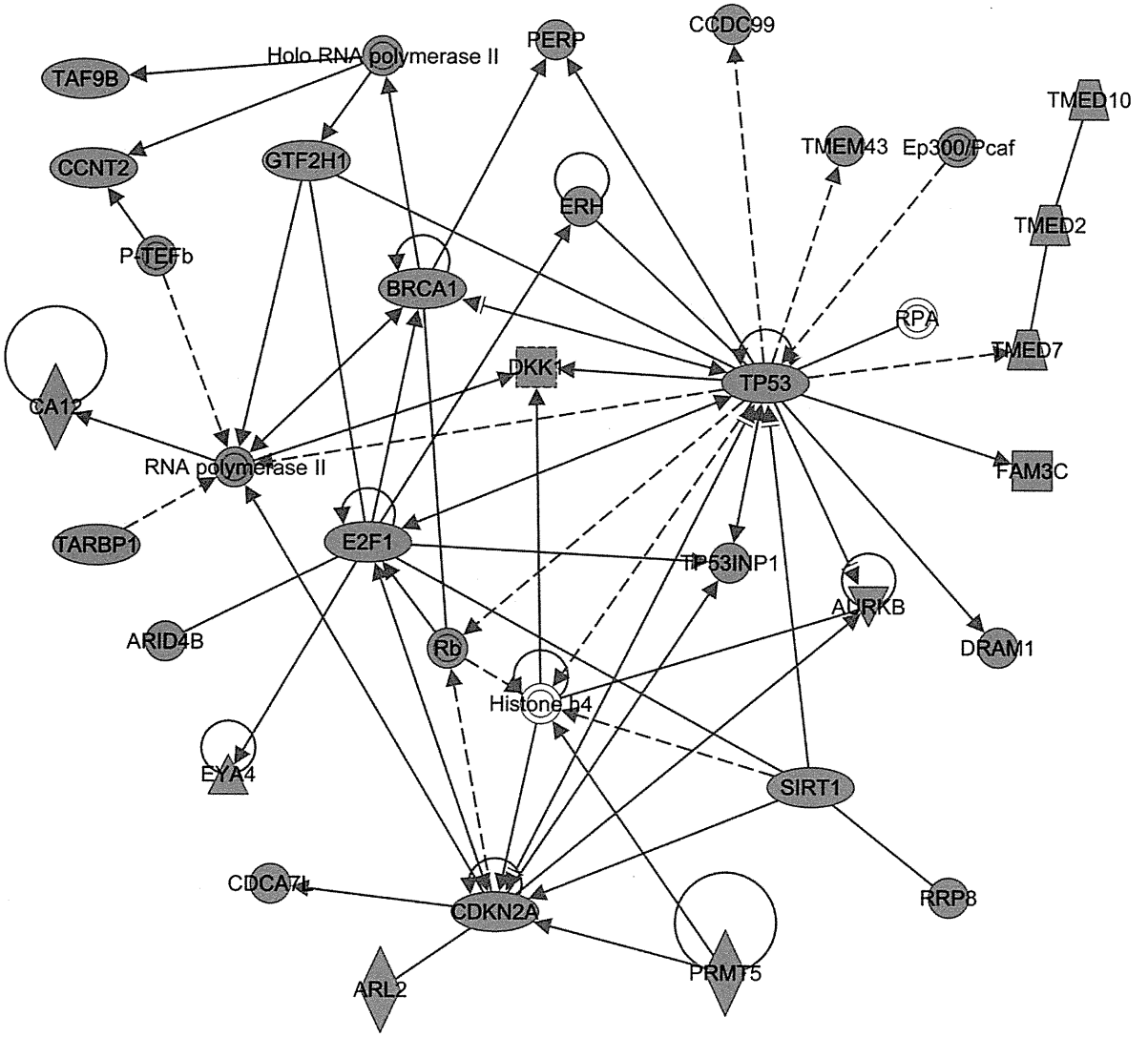

Fig. 2. Target genes for miRNAs downregulated in AD brains are located in the cell cycle-related network of IPA. The list of 852 target genes for the set of miRNAs downregulated in AD brains (Supplementary Table 1) was imported into IPA. Among the top 10 functional networks showing a significant association with target genes, the molecular network entitled "Cell cycle, connective tissue development and function, cellular growth and proliferation" (Rank 4 in Table 4) is illustrated. Target genes highlighted by red are potentially upregulated in AD brains.

Functional Annotation tool of DAVID, it identified a statistically significant association of the genes with several functional annotation categories (Table 2) and KEGG pathways (Table 3). The set of 852 genes showed a significant association with gene ontology (GO) terms related to regulation of cell proliferation, cell death, apoptosis, and cell cycle (Table 2). They also constructed KEGG pathways related to various types of cancers, cell cycle, focal adhesion, and signaling pathways of ErbB, p53, MAPK and TGF-beta (Table 3). Collectively, we concluded that a battery of cell cycle regulators, including cyclins, cyclin-dependent kinases (CDKs), cyclin-dependent kinase inhibitors (CDKIs), retinoblastoma protein (Rb), E2F family proteins, and p53, are highly enriched in both GO terms and KEGG pathways (Fig. 1).

Then, we validated the crucial involvement of cell cycle pathway in the molecular network of 852 target genes by uploading them into IPA and KeyMolnet. IPA suggested that these genes show a significant association with functional networks of cancer, cell growth, proliferation, development, and death, and cell cycle (Table 4). Again, major members of cell cycle regulators, including Rb, E2F1, and p53, are clustered in these networks (Fig. 2). KeyMolnet, based on the neighboring network-search algorithm, extracted a highly complex network composed of 3428 molecules and 6837 molecular relations, exhibiting a significant association with transcriptional regulation by a battery of transcription factors, such as Rb/E2F, cAMP responsive element binding protein (CREB), glucocorticoid receptor (GR), vitamin D receptor (VDR), NF-κB, hypoxia inducible factor (HIF), p53, and AP-1 (Fig. 3) (Table 5). Although the molecular pathways and networks illustrated by three different programs KEGG, IPA, and KeyMolnet armed with distinct computational algorithms do not perfectly merge each other, all the results supported the working hypothesis that the set of miRNAs downregulated in AD brains induces abnormal regulation of cell cycle progression via synchronous upregulation of multiple cell cycle regulators.

The cell cycle progression is positively and negatively regulated by the complex checkpoint mechanism. Increasing evidence convincingly shows aberrant expression of cell cycle regulators in the hippocampus, the basal forebrain, and the cerebral cortex of AD brains. They

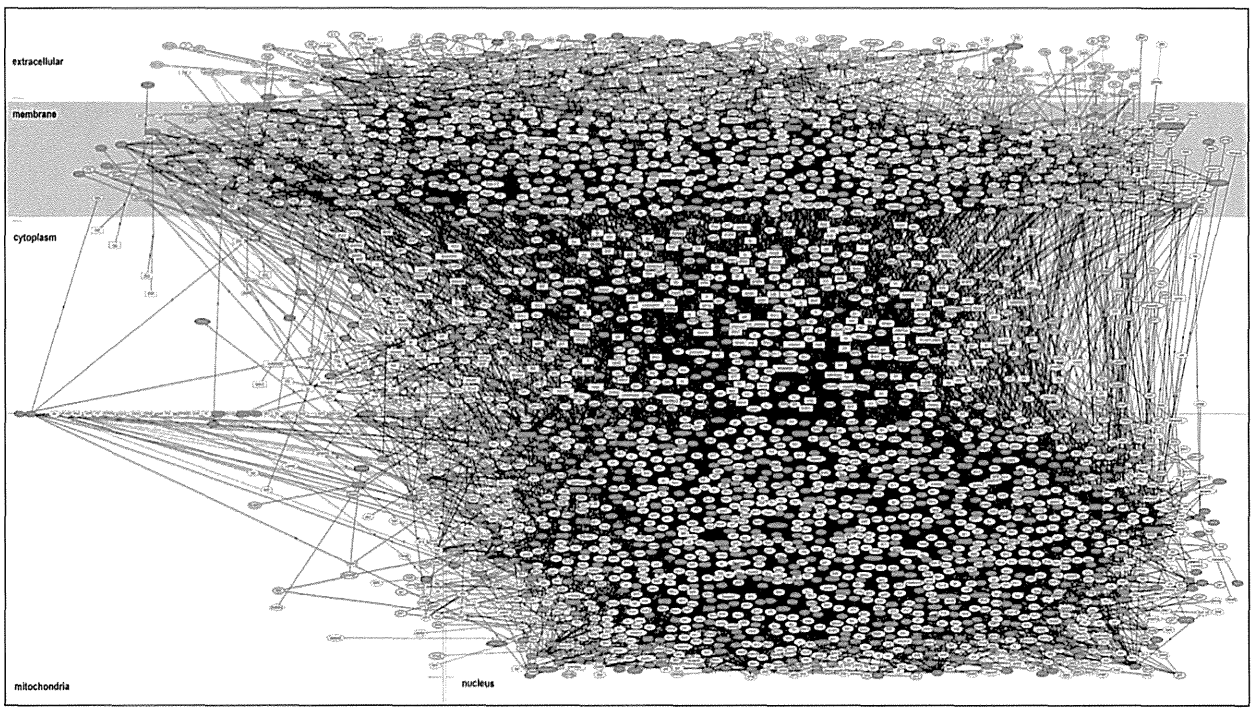

Fig. 3. KeyMolnet illustrates the highly complex molecular network of target genes for miRNAs downregulated in AD brains. The list of 852 target genes for the set of miRNAs downregulated in AD brains (Supplementary Table 1) was imported into KeyMolnet. The highly complex molecular network extracted by the neighboring network-search algorithm, composed of 3428 molecules and 6837 molecular relations, suggested the most significant relationship with the canonical pathway entitled "Transcriptional regulation by Rb/E2F" (Rank 1, Table 5). Target genes highlighted by red are potentially upregulated in AD brains.

include cyclins A, B, D, and E, along with CDKs and CDKIs of both the Cip/Kip and Ink4 families (Busser et al., 1998; McShea et al., 1997; Yang et al., 2003). The abnormal reentry into the cell cycle is an early event in neurons of AD brains stimulated by oxidative stress, which precedes Aβ deposition and NFT formation, and is potentially deleterious for terminally differentiated neurons, serving as a direct cause of neuronal apoptosis and degeneration (Bonda et al., 2010). The hypophosphorylated Rb protein interacts with the E2F family transcription factors E2F1, E2F2, and E2F3, and activates the expression of the genes pivotal for cell cycle progression, whereas the Rb protein, hyperphosphorylated by cyclin D1–CDK4 and cyclin E1–CDK2 complexes, releases E2Fs, and represses the expression of cell cycle genes (Swiss and Casaccia, 2010). Thus, the Rb/E2F pathway constitutes a molecular switch deciding either progression or arrest of the cell cycle. We found that RB1 is an experimentally validated target for miR-23b, 26a, 106a, 106b, 124a and 335, while E2F1 is a target for miR-17, 20a, 21, 23b, 93, 98, 106a, 106b, 223 and 330, E2F2 for miR-21, 24 and 98, and E2F3 for miR-34a, 34c and 195 (Supplementary Table 3). Thus, it is evident that E2F1 serves as one of hub molecules that play a central role in the cell cycle pathway. All of these miRNAs are downregulated in AD brains in the dataset of Wang et al. (Table 1), suggesting the logical hypothesis that the levels of expression of Rb and E2F proteins are abnormally elevated in AD brains (Figs. 1 and 2). Most importantly, aberrant expression of Rb protein and E2F1 is actually identified in neurons and glia cells in the frontal cortex of AD brains, where the Rb protein is hyperphosphorylated (Ranganathan et al., 2001).

Table 5
KeyMolnet pathways of target genes for miRNAs downregulated in AD brains.

Rank	KeyMolnet pathway	Score	Score p-value
1	Transcriptional regulation by Rb/E2F	882.46	2.25E-266
2	Transcriptional regulation by CREB	688.612	5.10E-208
3	Integrin family	630.668	1.41E-190
4	Transcriptional regulation by GR	508.344	9.40E-154
5	Transcriptional regulation by VDR	497.189	2.14E-150
6	Transcriptional regulation by NF-kB	495.71	5.98E-150
7	Transcriptional regulation by HIF	488.203	1.09E-147
8	TGF-beta family signaling pathway	387.147	2.87E-117
9	Transcriptional regulation by p53	386.348	4.98E-117
10	Transcriptional regulation by AP-1	367.719	2.02E-111

The list of 852 target genes for the set of miRNAs downregulated in AD brains was uploaded into KeyMolnet. It extracted a highly complex network composed of 3428 molecules and 6837 molecular relations, as illustrated in Fig. 3. The top 10 KeyMolnet pathways showing a significant association with target genes are listed with rank, KeyMolnet pathway, score, and p-value of the score. Abbreviations: Rb, retinoblastoma; CREB, cAMP responsive element binding protein; GR, glucocorticoid receptor; VDR, vitamin D receptor; NF-kB, nuclear factor kappa B; and HIF, hypoxia inducible factor.

In conclusion, we identified 852 experimentally validated target genes for the set of miRNAs downregulated in AD brains by searching them on the miRTarBase and UniGene. The molecular network analysis of 852 target genes by using three distinct pathway analysis tools of bioinformatics KEGG, IPA, and KeyMolnet proposed the system biological view that aberrant expression of cell cycle regulators might serve as a direct cause of neurodegeneration in AD brains.

Supplementary materials related to this article can be found online at doi:10.1016/j.expneurol.2011.09.003.

Acknowledgments

This work was supported by grants from the Research on Intractable Diseases, the Ministry of Health, Labour and Welfare, Japan (H22-Nanchi-Ippan-136; H21-Nanchi-Ippan-201; H21-Nanchi-Ippan-217; H21-Kokoro-Ippan-018) and the High-Tech Research Center

Project (S0801043) and the Grant-in-Aid (C22500322), the Ministry of Education, Culture, Sports, Science and Technology (MEXT), Japan.

References

Albert, R., Jeong, H., Barabasi, A.L., 2000. Error and attack tolerance of complex networks. Nature 406, 378–382.

Bettens, K., Brouwers, N., Engelborghs, S., Van Miegroet, H., De Deyn, P.P., Theuns, J., Sleegers, K., Van Broeckhoven, C., 2009. APP and BACE1 miRNA genetic variability has no major role in risk for Alzheimer disease. Hum. Mutat. 30, 1207–1213.

Boissonneault, V., Plante, I., Rivest, S., Provost, P., 2009. MicroRNA-298 and microRNA-328 regulate expression of mouse β-amyloid precursor protein-converting enzyme 1. J. Biol. Chem. 284, 1971–1981.

Bonda, D.J., Lee, H.P., Kudo, W., Zhu, X., Smith, M.A., Lee, H.G., 2010. Pathological implications of cell cycle re-entry in Alzheimer disease. Expert Rev. Mol. Med. 12, e19.

Busser, J., Geldmacher, D.S., Herrup, K., 1998. Ectopic cell cycle proteins predict the sites of neuronal cell death in Alzheimer's disease brain. J. Neurosci. 18, 2801–2807.

Cogswell, J.P., Ward, J., Taylor, I.A., Waters, M., Shi, Y., Cannon, B., Kelnar, K., Kemppainen, J., Brown, D., Chen, C., Prinjha, R.K., Richardson, J.C., Saunders, A.M., Roses, A.D., Richards, C.A., 2008. Identification of miRNA changes in Alzheimer's disease brain and CSF yields putative biomarkers and insights into disease pathways. J. Alzheimers Dis. 14, 27–41.

Cui, J.G., Li, Y.Y., Zhao, Y., Bhattacharjee, S., Lukiw, W.J., 2010. Differential regulation of interleukin-1 receptor-associated kinase-1 (IRAK-1) and IRAK-2 by microRNA-146a and NF-κB in stressed human astroglial cells and in Alzheimer disease. J. Biol. Chem. 285, 38951–38960.

Faghihi, M.A., Modarresi, F., Khalil, A.M., Wood, D.E., Sahagan, B.G., Morgan, T.E., Finch, C.E., St Laurent III, G., Kenny, P.J., Wahlestedt, C., 2008. Expression of a noncoding RNA is elevated in Alzheimer's disease and drives rapid feed-forward regulation of β-secretase. Nat. Med. 14, 723–730.

Faghihi, M.A., Zhang, M., Huang, J., Modarresi, F., Van der Brug, M.P., Nalls, M.A., Cookson, M.R., St-Laurent III, G., Wahlestedt, C., 2010. Evidence for natural antisense transcript-mediated inhibition of microRNA function. Genome Biol. 11, R56.

Filipowicz, W., Bhattacharyya, S.N., Sonenberg, N., 2008. Mechanisms of post-transcriptional regulation by microRNAs: are the answers in sight? Nat. Rev. Genet. 9, 102–114.

Fineberg, S.K., Kosik, K.S., Davidson, B.L., 2009. MicroRNAs potentiate neural development. Neuron 64, 303–309.

Friedman, R.C., Farh, K.K., Burge, C.B., Bartel, D.P., 2009. Most mammalian mRNAs are conserved targets of microRNAs. Genome Res. 19, 92–105.

Harraz, M.M., Dawson, T.M., Dawson, V.L., 2011. MicroRNAs in Parkinson's disease. J. Chem. Neuroanat. 42, 127–130.

Hébert, S.S., Horré, K., Nicolaï, L., Papadopoulou, A.S., Mandemakers, W., Silahtaroglu, A.N., Kauppinen, S., Delacourte, A., De Strooper, B., 2008. Loss of microRNA cluster miR-29a/b-1 in sporadic Alzheimer's disease correlates with increased BACE1/beta-secretase expression. Proc. Natl. Acad. Sci. U. S. A. 105, 6415–6420.

Hébert, S.S., Horré, K., Nicolaï, L., Bergmans, B., Papadopoulou, A.S., Delacourte, A., De Strooper, B., 2009. MicroRNA regulation of Alzheimer's amyloid precursor protein expression. Neurobiol. Dis. 33, 422–428.

Hébert, S.S., Papadopoulou, A.S., Smith, P., Galas, M.C., Planel, E., Silahtaroglu, A.N., Sergeant, N., Buée, L., De Strooper, B., 2010. Genetic ablation of Dicer in adult forebrain neurons results in abnormal tau hyperphosphorylation and neurodegeneration. Hum. Mol. Genet. 19, 3959–3969.

Hsu, C.W., Juan, H.F., Huang, H.C., 2008. Characterization of microRNA-regulated protein–protein interaction network. Proteomics 8, 1975–1979.

Hsu, S.D., Lin, F.M., Wu, W.Y., Liang, C., Huang, W.C., Chan, W.L., Tsai, W.T., Chen, G.Z., Lee, C.J., Chiu, C.M., Chien, C.H., Wu, M.C., Huang, C.Y., Tsou, A.P., Huang, H.D., 2011. miRTarBase: a database curates experimentally validated microRNA-target interactions. Nucleic Acids Res. 39, D163–D169.

Huang, da W., Sherman, B.T., Lempicki, R.A., 2009. Systematic and integrative analysis of large gene lists using DAVID bioinformatics resources. Nat. Protoc. 4, 44–57.

Kanehisa, M., Goto, S., Furumichi, M., Tanabe, M., Hirakawa, M., 2010. KEGG for representation and analysis of molecular networks involving diseases and drugs. Nucleic Acids Res. 38, D355–D360.

Kitano, H., 2007. A robustness-based approach to systems-oriented drug design. Nat. Rev. Drug Discov. 6, 202–210.

Kocerha, J., Kauppinen, S., Wahlestedt, C., 2009. microRNAs in CNS disorders. Neuromolecular Med. 11, 162–172.

Lukiw, W.J., 2007. Micro-RNA speciation in fetal, adult and Alzheimer's disease hippocampus. Neuroreport 18, 297–300.

Lukiw, W.J., Zhao, Y., Cui, J.G., 2008. An NF-κB-sensitive micro RNA-146a-mediated inflammatory circuit in Alzheimer disease and in stressed human brain cells. J. Biol. Chem. 283, 31315–31322.

Maes, T., Barceló, A., Buesa, C., 2002. Neuron navigator: a human gene family with homology to unc-53, a cell guidance gene from *Caenorhabditis elegans*. Genomics 80, 21–30.

Maes, O.C., Chertkow, H.M., Wang, E., Schipper, H.M., 2009. MicroRNA: implications for Alzheimer disease and other human CNS disorders. Curr. Genomics 10, 154–168.

McShea, A., Harris, P.L., Webster, K.R., Wahl, A.F., Smith, M.A., 1997. Abnormal expression of the cell cycle regulators P16 and CDK4 in Alzheimer's disease. Am. J. Pathol. 150, 1933–1939.

Mitchell, P.S., Parkin, R.K., Kroh, E.M., Fritz, B.R., Wyman, S.K., Pogosova-Agadjanyan, E.L., Peterson, A., Noteboom, J., O'Briant, K.C., Allen, A., Lin, D.W., Urban, N., Drescher, C.W., Knudsen, B.S., Stirewalt, D.L., Gentleman, R., Vessella, R.L., Nelson, P.S., Martin, D.B., Tewari, M., 2008. Circulating microRNAs as stable blood-based markers for cancer detection. Proc. Natl. Acad. Sci. U. S. A. 105, 10513–10518.

Nelson, P.T., Wang, W.X., 2010. MiR-107 is reduced in Alzheimer's disease brain neocortex: validation study. J. Alzheimers Dis. 21, 75–79.

Nelson, P.T., Wang, W.X., Rajeev, B.W., 2008. MicroRNAs (miRNAs) in neurodegenerative diseases. Brain Pathol. 18, 130–138.

Nelson, P.T., Dimayuga, J., Wilfred, B.R., 2010. MicroRNA in situ hybridization in the human entorhinal and transentorhinal cortex. Front. Hum. Neurosci. 4, 7.

Nunez-Iglesias, J., Liu, C.C., Morgan, T.E., Finch, C.E., Zhou, X.J., 2010. Joint genome-wide profiling of miRNA and mRNA expression in Alzheimer's disease cortex reveals altered miRNA regulation. PLoS One 5, e8898.

Ranganathan, S., Scudiere, S., Bowser, R., 2001. Hyperphosphorylation of the retinoblastoma gene product and altered subcellular distribution of E2F-1 during Alzheimer's disease and amyotrophic lateral sclerosis. J. Alzheimers Dis. 3, 377–385.

Satoh, J., 2010. MicroRNAs and their therapeutic potential for human diseases: aberrant microRNA expression in Alzheimer's disease brains. J. Pharmacol. Sci. 114, 269–275.

Satoh, J., Tabunoki, H., 2011. Comprehensive analysis of human microRNA target networks. BioData Min. 4, 17.

Satoh, J., Tabunoki, H., Arima, K., 2009. Molecular network analysis suggests aberrant CREB-mediated gene regulation in the Alzheimer disease hippocampus. Dis. Markers 27, 239–252.

Schratt, G.M., Tuebing, F., Nigh, E.A., Kane, C.G., Sabatini, M.E., Kiebler, M., Greenberg, M.E., 2006. A brain-specific microRNA regulates dendritic spine development. Nature 439, 283–289.

Selbach, M., Schwanhäusser, B., Thierfelder, N., Fang, Z., Khanin, R., Rajewsky, N., 2008. Widespread changes in protein synthesis induced by microRNAs. Nature 455, 58–63.

Sethi, P., Lukiw, W.J., 2009. Micro-RNA abundance and stability in human brain: specific alterations in Alzheimer's disease temporal lobe neocortex. Neurosci. Lett. 459, 100–104.

Shioya, M., Obayashi, S., Tabunoki, H., Arima, K., Saito, Y., Ishida, T., Satoh, J., 2010. Aberrant microRNA expression in the brains of neurodegenerative diseases: miR-29a decreased in Alzheimer disease brains targets neuron navigator-3. Neuropathol. Appl. Neurobiol. 36, 320–330.

Smith, P., Al Hashimi, A., Girard, J., Delay, C., Hébert, S.S., 2011. In vivo regulation of amyloid precursor protein neuronal splicing by microRNAs. J. Neurochem. 116, 240–247.

Swiss, V.A., Casaccia, P., 2010. Cell-context specific role of the E2F/Rb pathway in development and disease. Glia 58, 377–390.

Vasudevan, S., Tong, Y., Steitz, J.A., 2007. Switching from repression to activation: microRNAs can up-regulate translation. Science 318, 1931–1934.

Vilardo, E., Barbato, C., Ciotti, M., Cogoni, C., Ruberti, F., 2010. MicroRNA-101 regulates amyloid precursor protein expression in hippocampal neurons. J. Biol. Chem. 285, 18344–18351.

Viswanathan, G.A., Seto, J., Patil, S., Nudelman, G., Sealfon, S.C., 2008. Getting started in biological pathway construction and analysis. PLoS Comput. Biol. 4, e16.

Wang, W.X., Rajeev, B.W., Stromberg, A.J., Ren, N., Tang, G., Huang, Q., Rigoutsos, I., Nelson, P.T., 2008. The expression of microRNA miR-107 decreases early in Alzheimer's disease and may accelerate disease progression through regulation of β-site amyloid precursor protein-cleaving enzyme 1. J. Neurosci. 28, 1213–1223.

Wang, W.X., Huang, Q., Hu, Y., Stromberg, A.J., Nelson, P.T., 2011. Patterns of microRNA expression in normal and early Alzheimer's disease human temporal cortex: white matter versus gray matter. Acta Neuropathol. 121, 193–205.

Yang, Y., Mufson, E.J., Herrup, K., 2003. Neuronal cell death is preceded by cell cycle events at all stages of Alzheimer's disease. J. Neurosci. 23, 2557–2563.

Yao, J., Hennessey, T., Flynt, A., Lai, E., Beal, M.F., Lin, M.T., 2010. MicroRNA-related cofilin abnormality in Alzheimer's disease. PLoS One 5, e15546.

OPEN ACCESS Freely available online

PLOS | ONE

Plasmablasts as Migratory IgG-Producing Cells in the Pathogenesis of Neuromyelitis Optica

Norio Chihara[1,2], Toshimasa Aranami[1,6], Shinji Oki[1], Takako Matsuoka[1], Masakazu Nakamura[1], Hitaru Kishida[3], Kazumasa Yokoyama[4], Yoshiyuki Kuroiwa[3], Nobutaka Hattori[4], Tomoko Okamoto[5,6], Miho Murata[5], Tatsushi Toda[2], Sachiko Miyake[1,6], Takashi Yamamura[1,6*]

1 Department of Immunology, National Institute of Neuroscience, National Center of Neurology and Psychiatry (NCNP), Tokyo, Japan, **2** Department of Neurology, Kobe University Graduate School of Medicine, Kobe, Japan, **3** Department of Neurology, Yokohama City University Graduate School of Medicine, Yokohama, Japan, **4** Department of Neurology, Juntendo University Graduate School of Medicine, Tokyo, Japan, **5** Department of Neurology, National Center Hospital, NCNP, Tokyo, Japan, **6** Multiple Sclerosis Center, National Center Hospital, NCNP, Tokyo, Japan

Abstract

Neuromyelitis optica (NMO) is an inflammatory disease characterized by recurrent attacks of optic neuritis and myelitis. It is generally accepted that autoantibodies against aquaporin 4 water channel protein play a pathogenic role in neuromyelitis optica. We have recently reported that plasmablasts are increased in the peripheral blood of this autoimmune disease, and are capable of producing autoantibodies against aquaporin 4. Here, we demonstrate that $CD138^+HLA\text{-}DR^+$ plasmablasts, a subset of IgG-producing cells, are increased in the peripheral blood and are enriched among the cerebrospinal fluid (CSF) lymphocytes during the relapse of neuromyelitis optica. Notably, these $CD138^+HLA\text{-}DR^+$ plasmablasts overexpress CXCR3, whose ligands are present in the cerebrospinal fluid during the relapse of neuromyelitis optica. These results led us to speculate that plasmablasts producing anti-aquaporin 4 autoantibodies might traffic toward the central nervous system (CNS). Furthermore, we performed single-cell sorting of plasmablasts from peripheral blood and CSF samples from NMO and sequenced the complementarity-determining regions (CDRs) of the IgG heavy chain expressed by the sorted plasmablast clones. There were high frequencies of mutations in the CDRs compared with framework regions, indicating that these plasmablast clones would represent a post-germinal center B-cell lineage. Consistent with the preceding results, the plasmablast clones from the peripheral blood shared the same CDR sequences with the clones from the CSF. These results indicate that IgG-producing plasmablasts, which are guided by helper T-cells, may migrate from the peripheral blood preferentially to the CSF. Since migratory plasmablasts could be involved in the inflammatory pathology of NMO, the B-cell subset and their migration might be an attractive therapeutic target.

Citation: Chihara N, Aranami T, Oki S, Matsuoka T, Nakamura M, et al. (2013) Plasmablasts as Migratory IgG-Producing Cells in the Pathogenesis of Neuromyelitis Optica. PLoS ONE 8(12): e83036. doi:10.1371/journal.pone.0083036

Editor: Markus Reindl, Innsbruck Medical University, Austria

Received July 17, 2013; **Accepted** October 30, 2013; **Published** December 10, 2013

Funding: This work was supported by the Health and Labor Sciences Research Grant on Intractable Diseases (Neuroimmunological Diseases) from the Ministry of Health, Labor and Welfare of Japan (http://www.mhlw.go.jp/bunya/kenkyuujigyou/hojokin- koubo16/14.html; No.247), a Research Grant for Young Researcher from the Japan Multiple Sclerosis Society (http://www.jmss-s.jp; the award in 2011), a Research Grant on "Super Special Consortia" for Supporting the Development of Cutting-Edge Medical Care from the Cabinet Office (http://www.nanbyou.or.jp/entry/1512; No. 1512), Government of Japan, and a Grant-in-Aid for Scientific Research (S) from the Japan Society for the Promotion of Science (https://kaken.nii.ac.jp/d/p/18109009.ja.html; No. 18109009). The funders had no role in study design, data collection and analysis, decision to publish, or preparation of the manuscript.

Competing interests: TY serves as a guest editor (reviewer) for this journal. However, this does not alter the authors' adherence to all the PLOS ONE policies on sharing data and materials.

* E-mail: yamamura@ncnp.go.jp

Introduction

Neuromyelitis optica (NMO) is a rare inflammatory disease primarily affecting the optic nerve and spinal cord, with relatively sparing brain white matter [1]. NMO exhibits a relapsing–remitting course reminiscent of multiple sclerosis (MS) and was previously thought to be a variant of MS. However, NMO is now considered to have a unique pathogenesis characterized by the elevation of autoantibodies against aquaporin 4 (AQP4) [2,3]. NMO is more often accompanied by the elevation of serum autoantibodies including anti-nuclear, anti-SSA, and anti-SSB antibodies than MS. Notably, the relapses of NMO are not prevented but rather triggered by disease-modifying agents prescribed for MS, including interferon-beta[4,5]. Recent studies have indicated that primary autoimmune targets in NMO can be astrocytes, which abundantly express AQP4 in the end foot processes [6–8]. Consistently, inflammatory lesions of NMO are

surrounded by deposits of antibodies and complement that are associated with necrotic astrocytes, whereas AQP4 expression in astrocytes is downregulated in the early stage of NMO [6,7]. Moreover, large amounts of glial fibrillary acidic protein (GFAP) can be detected in the cerebrospinal fluid (CSF) of NMO patients during relapse [8]. Experimentally, systemic injection of large quantities of anti-AQP4 autoantibodies (AQP4Ab) from patients' sera exacerbated inflammatory pathology as well as clinical signs of experimental autoimmune encephalomyelitis in rats [9,10]. In this model of central nervous system (CNS) autoimmunity, the blood-brain barrier (BBB) integrity is disrupted following T-cell–mediated inflammation. In addition, similar astrocyte pathology was evoked in mouse brain by directly injecting AQP4Ab with human complement [11]. However, in human NMO, it remains unclear whether sufficient quantities of AQP4Ab may enter the CNS from the periphery so that they can cause the astrocyte pathology. This leaves room for a significant role of local production of AQP4Ab in the pathogenesis of NMO.

Recently, we reported that plasmablasts (PBs), bearing a phenotype of $CD19^{int}CD27^{high}CD38^{high}CD180^{-}$, are B-cells selectively increased in the peripheral blood of NMO, compared with control subjects [12]. A significant increase in PBs was observed during remission of NMO, but the increase was more remarkable during relapse in individual patients. Moreover, we identified the PBs as AQP4-Ab–producers in the peripheral blood of NMO. In principle, pathogen-activated B-cells migrate to lymphoid organs, and differentiate into PBs or memory B-cells (mB) within a germinal center. Some PBs move to the bone marrow and give rise to long-lived plasma cells, which contribute to maintaining the levels of serum antibodies against pathogens. The other PBs would die after undergoing apoptosis, or survive in lymphoid or non-lymphoid tissues in the inflammatory milieus [13]. However, the fate of the circulating PBs in the peripheral blood of NMO remains unclear.

The CSF of NMO patients reportedly contains much lower titers of AQP4-Ab than their peripheral blood [14], which is also supported by our unpublished results. On the other hand, cytokines preferring B-cell activation and survival, such as interleukin (IL)-6 or B-cell activating factor (BAFF), are elevated in the CSF of NMO patients [15,16]. Thus, low titers of AQP4-Ab in the CSF would not exclude the possibility of intrathecal AQP4-Ab production, but could reflect its deposition in inflammatory lesions. In this respect, the presence of AQP4-Ab–producing B-cells in the CSF was demonstrated in a patient with NMO [10], although the origin and identity of the cells were not fully characterized.

Here, we report that CSF lymphocytes obtained during the relapse of NMO are enriched in a subpopulation of PBs expressing CD138 and human leukocyte antigen (HLA)-DR ($CD138^{+}HLA\text{-}DR^{+}$ PB). These cells correspond to recently activated PBs, and also increase in the peripheral blood of patients with NMO during relapse. We found that during the relapse, the activated PB cells in the peripheral blood selectively upregulated CXCR3, a receptor for CXCL10 (interferon gamma-induced protein 10, IP-10) elevated in the CSF of NMO [17]. In contrast, PB expression of CXCR4, a receptor for bone marrow trafficking, was not altered during relapse. In parallel, we examined PB phenotypes in recently vaccinated healthy subjects. In these subjects, activated PBs increased significantly in number but did not upregulate either CXCR3 or CXCR4. These results led us to suspect that the upregulation of CXCR3 during the relapse of NMO might confer the PBs the ability to migrate to the CNS. Moreover, single-cell analysis of the antibodies variable region sequences revealed that the same complementarity-determining region (CDR) sequences in the γ chains were detected in PB clones derived from peripheral blood and from CSF. These results indicate that the $CXCR3^{+}$-activated PBs in the peripheral blood preferentially migrate to the CSF during the relapse of NMO and take part in the formation of the inflammatory pathology.

Materials and Methods

Ethics Statement

Informed consent was obtained from all participants after the nature and possible consequences of the studies were explained. The study was approved by the Ethics Committee of the each participated Institute or University; Ethics Committee of National Center of Neurology and Psychiatry, Ethics Committee for Medical Science of Kobe Graduate School of Medicine, Ethics Committee for Medical Research of Yokohama City University, and Ethics Committee of Juntendo University Hospital. Participants provided their written informed consent to participate in this study.

Patients and Controls

A cohort of 20 AQP4-Ab-seropositive patients was recruited at the National Center of Neurology and Psychiatry (NCNP) Hospital, Juntendo University Hospital, Yokohama City University Hospital, and Kobe University Hospital. Each patient either met the revised NMO diagnostic criteria [18] or was diagnosed with NMO spectrum disorder (NMOSD) [3]. Serum AQP4-Ab levels were measured with a previously reported cell-based assay using AQP4 transfectants, provided by courtesy of Dr. Kazuo Fujihara at Tohoku University [14]. Eight age-matched patients with MS were enrolled as controls. All MS patients fulfilled the McDonald diagnostic criteria [19]. Clinical demographics of the patients are summarized in Table **1**.

None of the seropositive patients or patients with MS had received intravenous (i.v.) corticosteroids, plasma exchange, or i.v. immunoglobulins for at least one month before blood or CSF sampling. Peripheral blood samples with or without CSF samples were obtained from seven seropositive NMO patients during relapse before they received intensive therapy such as i.v. corticosteroids. There were no significant differences among the NMO patients who provided samples during relapse or during remission, with regard to age, sex, disease duration, 2-year-relapse rate, expanded disability status scale (EDSS), and secondary prevention therapy. Peripheral blood was also taken from six healthy subjects before and one week after annual influenza vaccinations in 2010 to compare their PB cell phenotypes with those from NMO patients.

Table 1. The clinical profiles of patients with neuromyelitis optica (NMO)/NMO NMO spectrum disorder (NMOSD) and multiple sclerosis (MS).

Patients	NMO/NMOSD	MS
Number	20	8
Age	49.4 ± 3.9	43.0 ± 4.8
Male:Female	4:16	4:4
Disease duration	8.1 ± 2.0	9.9 ± 3.7
Relapses in the last 2 years	1.2 ± 0.3	2.3 ± 0.5
EDSS* score in disease remission	3.3 ± 0.5	4.1 ± 1.0

The values are expressed as the numbers or means ± standard error of the mean (SEM)

* Expanded disability status scale

doi: 10.1371/journal.pone.0083036.t001

Flow Cytometry Analysis and Cell Sorting

Peripheral blood mononuclear cells (PBMCs) were separated using density centrifugation on Ficoll-Paque PLUS (GE Healthcare Biosciences). CSF cells were directly stained for surface markers after centrifugation. FACSCanto II and FACSCalibur flow cytometers (BD Biosciences) were used for cell analysis along with the FACSAria II (BD Biosciences) cell sorter. We prepared samples with the same concentration of staining antibody and same fluorescence-activated cell sorting (FACS) setting (i.e., background autofluorescence control was set at the same levels and setting compensation was performed for each experiment using single-stained cells as compensation controls). The following monoclonal antibodies (mAbs) were used for flow cytometry analysis and cell sorting: anti-CD19 conjugated with electron-coupled dye (ECD), anit-CD38 conjugated with FITC, anti-HLA-DR conjugated with fluorescein isothiocyanate (FITC), anti-CD3 conjugated with FITC, and anti-CD138 conjugated with phycoerythrin (PE; Beckman Coulter); anti-CD38 conjugated with peridinin chlorophyll-protein complex (PerCP)-Cy5.5, anti-CD138 conjugated with PerCP-Cy5.5, anti-CD27 conjugated with Pacific Blue, anti-CXCR3 conjugated with PerCP-Cy5.5, anti-CXCR4 conjugated with biotin or with PE-Cy7-streptavidin (BioLegend); anti-CD19 conjugated with allophycocyanin (APC)-Cy7, anti-CD27 conjugated with PE-Cy7, anti-CD180 conjugated with PE, and anti-IgG conjugated with FITC (BD Biosciences); anti-CCR10 conjugated with APC; and anti-CXCR3 conjugated with FITC (R&D systems)

Sequencing Analysis of Immunoglobulin Gene Variable Regions

Since IgA-secreting PBs reportedly express CCR10 [20], we sorted CCR10^{-}PB cells □CD3^{-}CD19^{int}CD27^{high}CD38^{high}CD180^{-}CCR10^{-}□to obtain IgG-secreting PB cells. These PB cells were single-cell sorted into 96-well polymerase chain reaction (PCR) plates containing RNase inhibitor (Promega). We determined the variable region sequences of immunoglobulin genes in the sorted PBs according to a previously described protocol with some minor modifications [21]. Briefly, cDNA fragments of the variable regions of heavy chain (V_H) and light chain (V_{Kappa}) in each sorted cell were amplified by reverse transcription (RT)-PCR. High-fidelity Taq polymerase (Takara Bio) was used to avoid incorrect amplification. The reactions were followed by nested PCR using primer cocktails [21]. V gamma and V kappa cDNA fragments obtained from the first patient were cloned into pMD20-T vectors using Mighty TA-cloning reagents (Takara Bio). More than two clones derived from each single-cell sorted were sequenced to confirm the uniformity of the single PB sorting. Moreover, cDNA fragments of the V gamma genes obtained from another patient were directly sequenced using nested primer sets.

Data Analysis

Flow cytometry data were analyzed using the FlowJo software (Tomy Digital Biology). Statistical analysis was performed using Prism (GraphPad Software). In addition, Wilcoxon signed rank test, Mann–Whitney U test, or one-way analysis of variance (ANOVA) post-hoc test was used when appropriate.

Results

Predominance of PBs in CSF from NMO during relapse

We previously showed a significant increase of PB (CD19^{int}CD27^{high}CD38^{high}CD180^{-}) in the peripheral blood of NMO patients [12]. However, it remained unclear whether the PBs were also present in the CSF of NMO patients. In an extension study, we analyzed pairs of CSF and peripheral blood from NMO and MS patients. These samples were obtained during disease relapse. We have confirmed that CD27^{+} cells among CD19^{+} B-cells are more frequently found in the CSF (approximately 70%) than in the blood (30%) not only in MS but also in NMO (Figure **1A** and Figure **S1**). CD27 is a marker for mB carrying somatically mutated variable region genes [22]. More interestingly, the proportions of the PB cells were increased in the CSF lymphocytes from NMO compared to those from MS. In contrast, the proportions of mB (CD27^{+}CD38$^{low-mid}$CD180^{+} cells) tended to decrease reciprocally, even though it was not statistically significant (Figure **1B**). The proportions of the CD19^{+} B-cells and CD19^{+}CD27^{+} B-cells among the PBMC and CSF were not different between NMO and MS patients (Figure **S2**). However, the frequency of PB cells among CD19^{+} B-cells increased significantly in the peripheral blood and CSF of NMO patients compared to that of MS patients (Figure **S3**). An additional study on three NMO patients during remission did not reveal the presence of PBs in the CSF, despite the presence of mB. Therefore, we speculated that the PB cells in the CSF might play an active role during the relapse of NMO.

PB cells infiltrating CNS are CD138^{+}HLA-DR^{+}

We asked whether a particular PB subset might exhibit more drastic changes than the whole PB cells. Then, we analyzed the phenotypes of PB subpopulations in the peripheral blood, using antibodies against CD138 and HLA-DR. We showed previously that some PBs in NMO would express the plasma